AD-A125 846 AMPLITUDE AND PHASE OF SURFACE PRESSURE PRODUCED BY SPACE TRANSPORTATION SYSTEM - MISSION 5(U) WESTON OBSERVATORY MA F A CROWLEY ET AL. JAN 83 1/1

UNCLASSIFIED AFGL-TR-83-0039 F19628-81-K-0005 F/G 22/4 NL

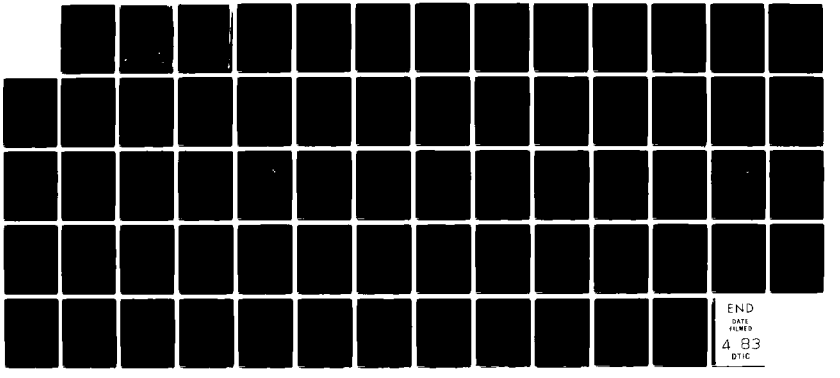

END
DATE FILMED
4 83
DTIC

1/1

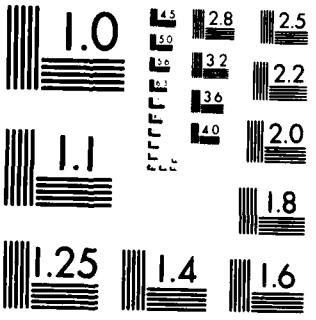

MICROCOPY RESOLUTION TEST CHART
NATIONAL BUREAU OF STANDARDS 1963 A

[redacted]

Francis J. Crossley
Eugene R. Hartnett
Henry A. Oesing

Weston Observatory
Department of Geology and Geophysics
Boston College
381 Concord Road
Weston, Massachusetts 02193

January 1983

Scientific Report No. 3

Approved for Public Release; Distribution Unlimited

Air Force Geophysics Laboratory
Air Force Systems Command
United States Air Force
Hanscom AFB, Massachusetts 01731

Unclassified

SECURITY CLASSIFICATION OF THIS PAGE (When Data Entered)

REPORT DOCUMENTATION PAGE		READ INSTRUCTIONS BEFORE COMPLETING FORM
1. REPORT NUMBER AFGL-TR-83-0039	2. GOVT ACCESSION NO. A125 846	3. RECIPIENT'S CATALOG NUMBER
4. TITLE (and Subtitle) Amplitude and Phase of Surface Pressure Produced by Space Transportation System - Mission 5		5. TYPE OF REPORT & PERIOD COVERED Scientific Report No. 3 Nov 82 - Jan 83 6. PERFORMING ORG. REPORT NUMBER
7. AUTHOR(s) Francis A. Crowley Eugene B. Hartnett Henry A. Ossing *		8. CONTRACT OR GRANT NUMBER(s) F19628-81-K-0005
9. PERFORMING ORGANIZATION NAME AND ADDRESS Weston Observatory, Department of Geology and Geophysics, Boston College, 381 Concord Road, Weston, MA 02193		10. PROGRAM ELEMENT, PROJECT, TASK AREA & WORK UNIT NUMBERS 62101F 7600-09 AD
11. CONTROLLING OFFICE NAME AND ADDRESS Air Force Geophysics Laboratory Hanscom AFB, MA 01731 Contract Manager: Henry A. Ossing/ LWH		12. REPORT DATE January 1983 13. NUMBER OF PAGES 65
14. MONITORING AGENCY NAME & ADDRESS(if different from Controlling Office)		15. SECURITY CLASS. (of this report) UNCLASSIFIED 15a. DECLASSIFICATION/DOWNGRADING SCHEDULE

16. DISTRIBUTION STATEMENT (of this Report)

APPROVED FOR PUBLIC RELEASE - DISTRIBUTION UNLIMITED

17. DISTRIBUTION STATEMENT (of the abstract entered in Block 20, if different from Report)

18. SUPPLEMENTARY NOTES

Block 7- * Air Force Geophysics Laboratory

19. KEY WORDS (Continue on reverse side if necessary and identify by block number)

Rocket Plume Acoustics
Acoustic Coupling
STS Seismic - Acoustic Fields
STS Launch Environment

20. ABSTRACT (Continue on reverse side if necessary and identify by block number)

Surface pressures produced at distances of 150-300 meters from the launch of STS-5 are analyzed. The calculated attenuation, phasing and spacial coherence of surface pressure observations are consistant with the pressure produced by acoustics propagating outward from a single, small source moving with the rocket. The OASPL estimates for STS-5, calculated from standard form spectra, point to low acoustic efficiency or axially asymmetric acoustics for the shuttle.

DD FORM 1 JAN 73 1473 EDITION OF 1 NOV 65 IS OBSOLETE

UNCLASSIFIED

SECURITY CLASSIFICATION OF THIS PAGE (When Data Entered)

TABLE OF CONTENTS

AMPLITUDE AND PHASE OF SURFACE PRESSURE PRODUCED BY SPACE TRANSPORTATION SYSTEM - MISSION 5

1.0 INTRODUCTION

1.1 Statement of Need

There is a need to forecast the vibro-acoustic environment for Space Transportation System (STS) launches at Vandenberg (VAFB). Previous data were inadequate to establish the phase of the launch pressure on major close-in structures at Launch Complex 6, VAFB. Specification of phase is essential to vibration forecasts. Model responses of VAFB structures have been found to be extremely sensitive to the phase of the applied load.

1.2 Immediate Aim of Work

To correct this deficiency, array measurements of surface pressure were taken of STS-5. These data permit a determination of the amplitude and phase of pressure excited by an STS launch over an area and at an orientation and distance of interest to Space Division. The measurements are used to construct and test a point source model to represent launch pressure. Of particular concern to vibration forecasts here is the level spacial coherency and effective source height for plume generated pressures at a range of 150-300 meters.

2.0 FINDINGS

Overall Sound Power Level (OASPL) calculations for surface measurements taken in line with the Columbia's vertical stabilizer are unexpectedly low (prelaunch configuration).

STS-5 launch generated surface pressures are coherent in the

sense that at any one time a unique amplitude and phase factor exists to connect pressure observations separated by a spacial shift, $\vec{\Delta}R$.

Calculated phase, attenuation and (spacial) coherency values for surface pressures generated by the STS-5 launch are entirely consistent with a surface pressure produced by an acoustic disturbance propagating outward from a single, small source moving with the rocket.

3.0 CONCLUSIONS

The low pressure level found here indicates that the STS OASPL is asymmetric about the rocket's body axis.

An "equivalent point source", essential to vibration forecasts can be constructed from the Kennedy Space Center(KSC) data to control facility response measurements at VAFB.

The location and construction of an axially asymmetic source permits a forecast of site peculiar pressures at VAFB due to reflections off structures and topography.

4.0 THE MEASUREMENT SYSTEM

The measurement system (GDAS) used here is an Air Force Geophysics Laboratory (AFGL) developed unit that collects, displays, stores and analyzes geophysical data. A detailed description of GDAS has been given by von Glahn (1). Since his report the GDAS has been upgraded to include better amplifiers, a faster central processing unit, expanded memory, Winchester disc storage, electrostatic graphics and remote control. The remote control feature was added to take measurements at KSC.

4.1 Sensor Locations

In its configuration at KSC as shown in Figure 1, GDAS accepts the output of an array of 12 pressure sensors. Each observable is converted into a 12 bit binary word at a rate of 100 conversions per second. These data are merged with identification, error suppression, time and status codes for storage on magnetic tape with a backup dump to disk. Measurements of Mission 5 start 3 minutes prior to lift-off and continue for a period of 15 minutes.

The orientation, size and distance to the array mirrors the orientation, size and distance to major structures at VAFB. The array is configured to determine the level, phase and spacial coherency of the acoustic load at the time of the sound power level maximum for large structures at a range of 150-300 meters.

It should be recognized that the vibro-acoustics around pad 39A at KSC will consistently differ from those at VAFB. The launch environment reflects a number of site dependent parameters. If the geology, topography and structures at the two sites are quite dissimilar, the vibro-acoustics will differ. In contrast, the "equivalent source" we seek is insensitive to site. Indeed, a major justification for constructing an "equivalent source" is to isolate and treat the effects introduced by site peculiar features.

4.2 Data Quality

A number of error sources that determine the quality of measurement are now explicitly considered. This heightened concern about data quality is prompted by the fact that the pressure values reported here are significantly smaller than those measured by

NASA (2) and anticipated for a propulsion system of standard acoustic efficiency (3).

4.2.1 Sensor Scale Factors and Channel Gains

Table 1 summarizes a verification of sensor scale factors and channel gains. Individual test waveforms and channel parameters used to construct the table are carried in Appendix A. Sensor scale factors were determined before and after the launch at D&J Instruments, Inc. in Billerica, Massachusetts. The standard single measurement accuracy claimed by this facility is ¼%. Amplifier gains were established by measurements of the GDAS as deployed at KSC. Scatter in peak-to-peak pressure values in tests using a common input pressure is less than 1%.

In Figure 2 the overall response that satisfies the sensor and amplifier values of Channel 6 are shown to twice the Nyquist frequency, f_N=50 Hz. As can be seen, first-fold alias terms are down by more than two orders of magnitude for frequencies less than 30 Hz.

TABLE 1

Pressure Response Test # 8 - 11 Nov 82 1240 EST

Ch #	V_o(P-P) VOLTS	Sensor ScF VOLTS/PSI	AMP GAIN	P(P-P) PSI
1	2.357	2.940	5.04	.159
2	3.477	4.402	4.94	.160
3	2.208	2.762	5.09	.157
4	3.671	4.581	5.04	.159
5	2.935	3.813	4.93	.156
6	2.898	3.625	5.01	.160
7	2.783	3.551	5.00	.157
8	2.507	3.208	5.00	.156
9	2.239	2.917	4.89	.157
10	2.577	3.238	5.06	.157
11	2.561	3.295	4.92	.158
12	2.846	3.595	5.02	.158

For completeness, we have included all measurements taken in this study for an interval starting at 0718:55 EST and continuing for 35 seconds, Appendix B. The conspicuous transient at 0719:01 is due to the ignition of the solid booster rockets. Other events of interest are noted with the observations.

4.2.2 Uncorrelated Additive Noise

Measurements taken on channels 7 and 12 are used to isolate additive noise caused by atmospheric and hardware sources from those due to launch generated acoustics. For acoustic inputs, the sensors are close enough to one another to be treated as common. In contrast, voltages excited by small, slow moving eddies and hardware sources are largely uncorrelated both between channels and with the acoustic load produced by the propulsion system. Figure 3 is the total and incoherent spectra obtained for low level measurements. The spectral estimates shown here use periodogram smoothing that calls for interval doubling by concatenating zeros to the original data set. The technique reduces the variance of the estimate and suppresses spectral leakage (4). Coherency estimates, Figure 4, used to separate the spectra are based on auto and cross spectra calculations on 10 data segments (5). The signal-to-noise estimate for low level measurements shown in Figure 5 is the ratio of the square root of the coherent and incoherent spectra.

The confidence bounds for S/N values calculated from coherency estimates have been determined by Fay (6) for a stationary, Gaussian process. For coherencies as large as those shown in Figure 4 at frequencies of 30 Hz or less, stable coherency and S/N estimates can be obtained by ensemble averaging over a small sample set. To illustrate, the interval for a coherency estimate, Coh (f) = 0.9, based on an ensemble average of 8 samples, is calculated to be $0.8 \leq \text{Coh} \leq 0.96$ at the 95% confidence level for Gaussian variates.

The entire sequence used to estimate the dynamic range of GDAS

at low measurement levels is repeated for high level measurements. The results are shown in Figures 6-8. We conclude that the signal-to-noise level for an individual channel is typically well in excess of 10 in the bandpass $2 \leq f \leq 30$ Hz for modest level observations. For frequencies above 30 Hz, measurements are substantially degraded by an additive, uncorrelated noise term.

4.2.3 Signal Induced Noise

A number of signal induced noise terms can arise due to system non-linearities and digitization. System linearity and digitization accuracy are regularly verified at the 1% level by inserting known signals into GDAS.

Another obvious area of concern for operating GDAS at KSC was spurious terms arising from vibration. A sequence of performance tests was conducted with GDAS affixed to a two axis shake table at the Acton Environmental Testing Corporation, Acton, Massachusetts just prior to shipment to KSC (7). No motion induced noise terms were found for vibration levels as high as 0.5 g's. Both the level and duration of the motion in these certification tests are well in excess of the motion experienced by GDAS during the launch of STS-5.

5.0 ANALYSIS OF SURFACE PRESSURE

5.1 Main Engine

The analysis of main engine acoustics is based on data samples of 2.56 seconds duration starting at 0718:57. The pressure spectrum given in Figure 9 is a periodogram average of seven samples taken at locations 3-6 and 8-10 inclusive, see Figure 1. For frequencies below 30 Hz,

the spectrum is well separated from system noise determined for low level measurements. Much above 30 Hz, the data are dominated by uncorrelated, additive noise. Below 2 Hz, pressure fluctuations expected for the 5 knot wind reported at the time of launch rapidly become a significant factor. A spectrum of pressure fluctuations for a 5 knot wind condition reported by Kimball (8) is included in Figure 9.

The pressure, p(R,t) caused by an acoustic disturbance propagating outward from a small source located at the origin of a windless, isothermal, unbounded atmosphere is completely coherent along any radial segment with an amplitude and phase determined from its Fourier transform.

$$p(R,\omega) = p(\omega) \cdot \frac{1}{R} \exp i \left\{ kR + \phi_s \right\} \qquad k = \omega / C_a \quad R > 0$$

C_a is the speed of sound in air and ϕ_s is a phase term at the source. In contrast, distributed, independent sources invariably lead to incoherent fields for separated observers. The magnitude of the coherence loss generally increases with the magnitude of the separation.

Main engine pressure measurements, $p(r_\ell, t)$ at distances $r_\ell \ell = 1,2,\ldots 12$ are taken to be a spacially coherent acoustic term corrupted by independent additive noise. Under this construction the magnitude of the ratio of k weighted vector and scalar sums of $p(r,\omega)$, the transformed pressure measurements corrected for hardware response are given by:

$$\gamma(k,\omega) = \left| \frac{\sum_{\ell=1}^{12} p(r_\ell,\omega) e^{ikr_\ell}}{\sum_{\ell=1}^{12} \left| p(r_\ell,\omega) \right|} \right|$$

For a coherent acoustic field, $\nu(k, \omega)$ approaches unity for large S/N measurements when $C_a = \omega/k$ and $\omega = 2\pi f$.

Figure 10 is a plot of the absolute maxima of $\nu(k', \omega)$ for k weighted Fourier coefficients of the measured pressure samples. In the band where additive noise is small, the magnitude is close to unity. The measured pressures are coherent under a phase shift given by $(k'r_\ell = \omega\tau_p)$.

Figure 11 locates the (k, ω) pairs to obtain absolute maxima $\nu(k, \omega)$ values. The plot establishes the propagation characteristics for main engine pressure over the array. The phase velocity, C, calculated directly from (k, ω) pairs is given in Figure 12. The median C value for frequencies in the band $2 \leq f \leq 30$ Hz is 350.6 meters/second. Within this frequency band, surface pressure measurements are well represented by a coherent, non-dispersive, acoustic disturbance propagating outward from a single small source region located near the launch pad. For frequencies much above f = 30 Hz the scatter both in $\nu(k, \omega)$ and $C(\omega)$ are consistent with errors due to measurement noise. There is no need to interpret the scatter as a breakdown in the single source characteristic of the pressure field.

5.2. Solids Ignition Pulse

The ignition of the solid engines produced a conspicuous transient over the array at 0719:01. The power spectral density for a 2.56 second time gate starting at 0719:00.25 EST that includes the ignition transient is given in Figure 13. The spectrum is computed in the same fashion and over the same station set as before for constructing Figure 9. The energy spectrum of the transient resulting

from the ignition of the solid engines peaks below 3 Hz.

We again establish the spacial coherency and phase velocity of the sample by locating the absolute maxima of $\gamma(k, \omega)$ over trial sets of k values, see Figures 14,15. The ignition pressure is found to propagate over the array as a coherent, non dispersive disturbance at a velocity of 347 meters/second.

As well recognized by NASA, the need to predict pressure spacially is essential to vibration forecasts for large class structures (9). Figure 16 illustrates how well we can spacially predict pressure from phase shifts obtained from (k, ω) pairs and 1/R attenuation. Trace 1 is the pressure value measured 293 meters south of the launch pad starting 0.25 seconds after launch. Trace 2 is an average of all the measurements corrected for differences in amplitude (1/r attenuation), phase (ikr_ℓ) and hardware response. The error trace is the residue that cannot be represented by a spherically divergent acoustic term incident on a smooth ground of constant reflectivity. The residual term, Trace 3, is quite small.

Clearly, secondary sources arising from reflections off structures and topography are minimal at KSC. Almost the entire measurement is satisfied by outward propagating acoustics and additive hardware noise. (This finding continues to be true over the entire launch sequence). Pressure predictions at VAFB, in contrast, must anticipate secondary sources caused by reflections from a number of major structures. The launch pressure environment at the two sites will differ.

5.3 Plume Sound Level Maximum

A major objective of this effort is the determination of the magnitude, phase and coherence of launch generated pressure around the time of maximum loading over distances and azimuths to major structures at VAFB. For our measurements of STS-5 the maximum occurs some 11 seconds after lift-off. At this time the plume is taken to be close to vertical and in an undeflected, steady-state condition. The vehicle has just commenced its roll maneuver. Water suppression is now assumed (perhaps incorrectly) to be ineffective for attenuating pressure in the array area.

The average spectrum, Figure 17, for surface measurements south of the shuttle (aligned with the Columbia's vertical stabilizer) over the same station set as before is well above additive noise for frequencies less than 35 Hz. For higher frequencies, measurements are probably contaminated by digital noise, as well as additive noise. The measured spectrum has the usual bell shape when plotted in log-log format (10). A spectral maximum somewhat in excess of 130 db is found around 5 Hz. The S/N estimate for measurements near the maximum is in excess of 100.

As before, the single source nature of the pressure field is determined by $\hat{\gamma}(k, \omega)$ calculations, Figure 18. For times around the maximum, $\hat{\gamma}(k, \omega)$ typically remains well in excess of the half power level (.707). Pressures, particularly near the 5 Hz spectral maximum are well represented by a spacially coherent, acoustic disturbance. This feature continues to hold true for surface pressures well after lift-off. At these later times there is some evidence of dispersion that is consistent with the notion that the longer waves "appear to "

originate from a point lower in the plume.

Figure 19 summarizes phase velocity estimates for the STS-5 launch calculated from (k, ω) pairs located by absolute $\gamma(k, \omega)$ maxima. Around the load maximum, STS pressures can be modeled by acoustics coming from a small source located some 100-150 meters above the launch pad.

6.0 PLUME SPECTRA IN STANDARD FORM

After Hartnett, (11) we construct stable broadband spectral estimates of surface pressure by fitting periodograms to the spectral form advocated by Powell (12) for undeflected, plume generated acoustics. The spectrum

$$G_{pp}(f) = \frac{4}{\pi} \frac{OASPL}{f_m} \left\{ f/f_m + f_m/f \right\}^{-2}$$

is fitted to periodograms by selecting values of OASPL and f_m, the frequency at the spectral maximum, that minimize the square of the residuals between periodogram coefficients and $G_{pp}(f)$. The best fitting spectrum for data starting at 11 seconds after lift-off is shown in Figure 20.

It is worth noting that periodgram values given in Figure 20 are only modestly lower than those forecast for frequencies less than f_m. At frequencies greater than $2f_m$, the calculated coefficients are an order of magnitude lower. The theoretical overall acoustic power calculated for STS-5 is found to be less than that measured for a Titan III-D, a vehicle with a thrust level less than half that of the shuttle (3).

Table 2 is a set of OASPL and f_m values that best fit data samples for times shortly after launch. The maximum OASPL for a surface measurement at 293 meters occurs 11 seconds after lift-off. The OASPL is calculated to be 139 db. The spectrum is a maximum at 4.37 Hz.

TABLE 2: STANDARD SPECTRA PARAMETERS

(for 293 Meters)

Time After Lift-Off (Seconds)	fm Hz	OASPL PSI^2		Figure of Merit	OASPL (db)
6	10.86	2.652	$*10^4$	325.9*	135
9	4.96	6.381	"	1.23	139
11	4.37	6.982	"	0.84	139
14	2.79	4.429	"	0.54	137
17	2.49	1.459	"	1.41	132
20	3.89	1.011	"	0.94	131

* Periodogram does not fit STANDARD FORM.

Two tests were run to evaluate when the calculated periodograms could be represented by a stochastic process with a spectra of the form

proposed by Powell. One such test is shown in Figure 21. The figure plots the observed residuals against the residual distribution of a Chi squared variate with DOF=2, the expected distribution, had we fitted periodogram ordinates to the true spectra. The plot is constructed to make the acceptance criteria one of simply accepting the residuals to lie on the indicated straight line. Both by this test and a test based on the acceptance range for a figure of merit established by Hartnett, we conclude that the calculated periodograms are well represented by a spectrum of the form $G_{pp}(f)$ for all but the data starting 6 seconds after lift-off. This early in the launch the acoustics do not exhibit the spectral form ascribed to an undeflected plume (and probably rightly so).

7.0. COMPARISON TO FORECASTED VALUES HELD

It has long been widely accepted that the acoustic efficiency of an undeflected rocket exhaust, defined by the ratio of the OASPL to the exhaust's mechanical power, is about 0.5%, independent of thrust level (10). Indeed, the simple linear relation between maximum OASPL and thrust for an observer at a fixed distance over the wide range of thrust levels shown in Figure 22 was the basis for AFGL's early forecasts for shuttle launches at VAFB (13). The forecast assumed that the OASPL is axially symmetric about the rocket's body axis. Consequently, surface pressure for a vertical rocket was expressed solely as a function of distance.

In Figure 22, the OASPL calculated for STS-5 appears to be quite low. The "apparent" acoustic efficiency of this rocket is substantially

lower than that of most large class rockets. Further, the location of the spectral maxima forecast for f_m based on a Strouhal number that is in harmony with the STS engine parameters also differs from the value forecast (3).

8.0 REFERENCES

1. Von Glahn, P.G., The Air Force Geophysics Laboratory Standalone Data Acquisition System: A Functional Description, AFGL-TR-80-0317, Oct 1980.

2. NASA Report No. KSC-DD-457-TR, Space Shuttle STS-1 Launch Processed Ground Measurements, Vol I, Sep 1981.

3. Crowley, F.A., Hartnett, E.B. and Ossing, H.A., The Seismo-Acoustic Disturbance Produced by a Titan III-D with Applications to the Space Transportation System Launch Environment at Vandenberg AFB, AFGL-TR-80-0358, Nov 1980.

4. Yuen, C.K., On The Smoothed Periodogram Method for Spectrum Estimation, Signal Processing Vol I, No. 1, Jan 1979.

5. Bendat, J. and Piersol, A., Measurement and Analysis of Random Data, John Wiley and Sons, 1966.

6. Fay, J.W., Confidence Bounds for Signal-to-Noise Ratios from Magnitude Squared Coherence Estimates, IEEE Transactions on Acoustics, Speech and Signal Processing, Vol. ASSP-28, No. 6, Dec 1980.

7. Acton Environmental Testing Corp Test Report No. 17818-83D, Sine Sweep Testing of a Monitoring Computer System, Oct 1982.

8. Kimball, B.A. and Lemon, E.R., Spectra of Air Pressure Fluctuations at the Soil Surface, JGR Vol 75, No. 33, Nov 1970.

9. NASA Report No. GP-1059, Revision A, Environment and Test Specification Levels Ground Support Equipment for Space Shuttle System Launch Complex 39, Acoustic and Vibration, Vol. I, Sep 1976.

10. NASA Report No. Sp-8072, Acoustic Loads Generated by the Propulsion System, 1971.

11. Hartnett, E. and Carleen, E., Characterization of Titan III-D Acoustic Pressure Spectra by Least Squares Fit to Theoretical Model, AFGL-TR-80-0004, Jan 1980.

12. Powell, A., Theory of Vortex Sound, Jour Acous Soc of America Vol. 36, No. 1, Jan 1964.

13. Crowley, F.A., Hartnett, E.B. and Chen, K., Ground Vibration Level Estimates for Space Transportation System Launces at Vandenberg AFB, AFGL-TR-77-0083, 28 Mar 1977.

9.0 ILLUSTRATIONS

Figure Title

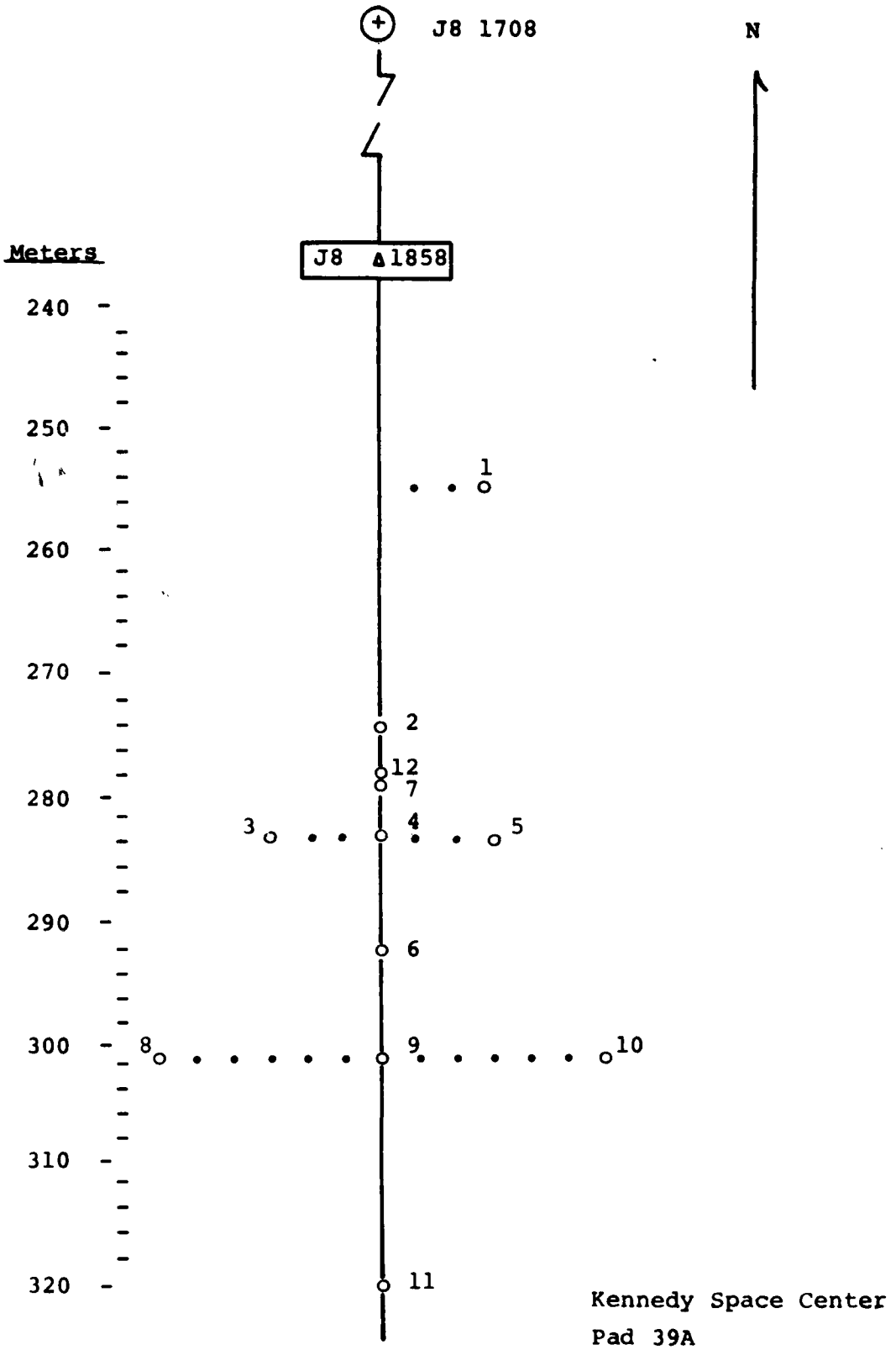

SENSOR LOCATIONS

Figure 1

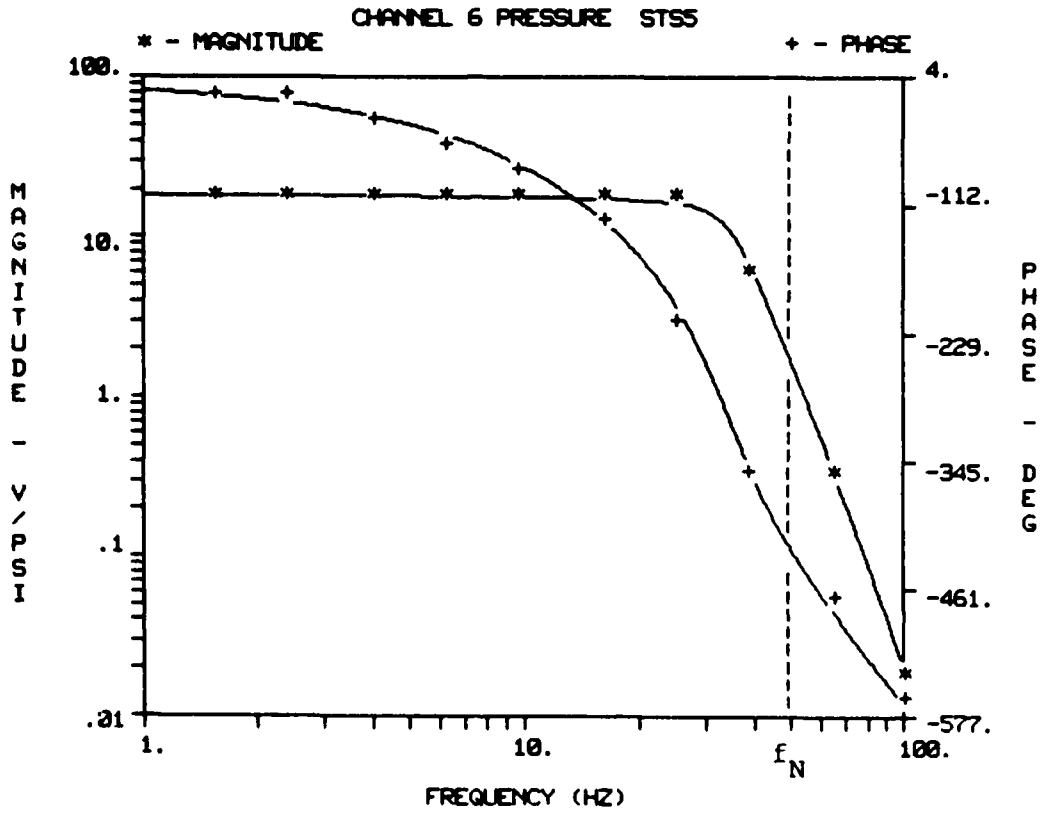

CHANNEL RESPONSE

Figure 2

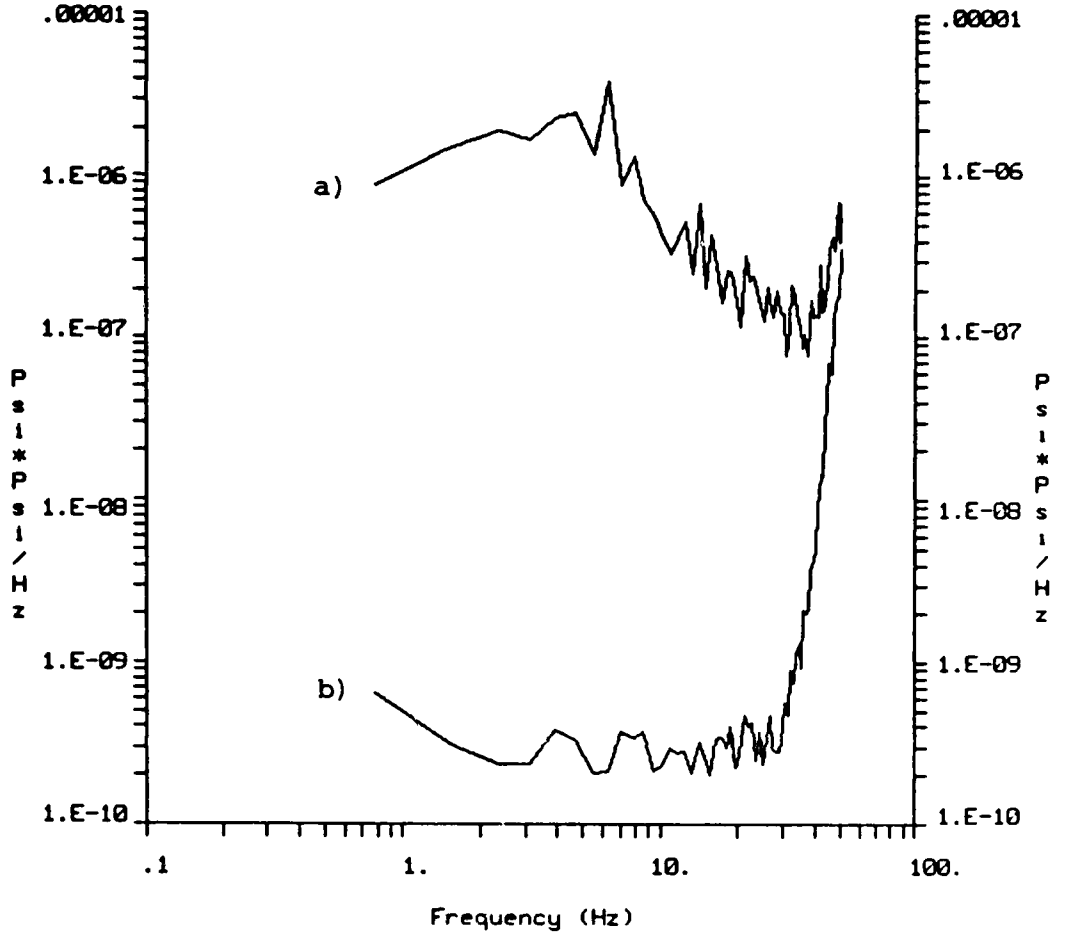

DOF=20

a) Total Spectra

b) Incoherent Portion

PRESSURE SPECTRA (LOW LEVEL)

Figure 3

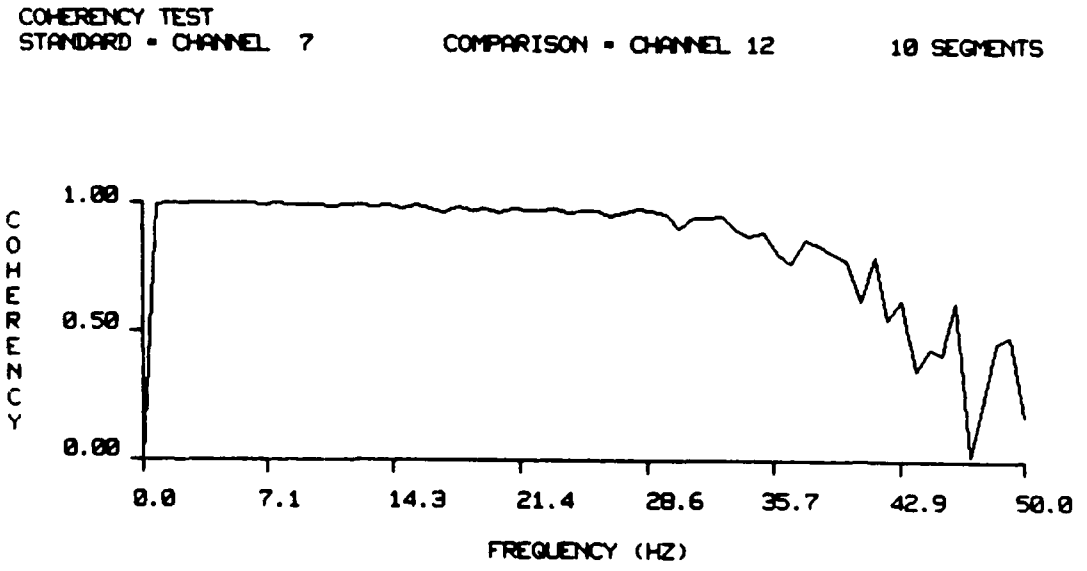

Sensor Separation ≈ 1 Meter

CHANNEL COHERENCY
LOW LEVEL PRESSURE MEASUREMENTS

Figure 4

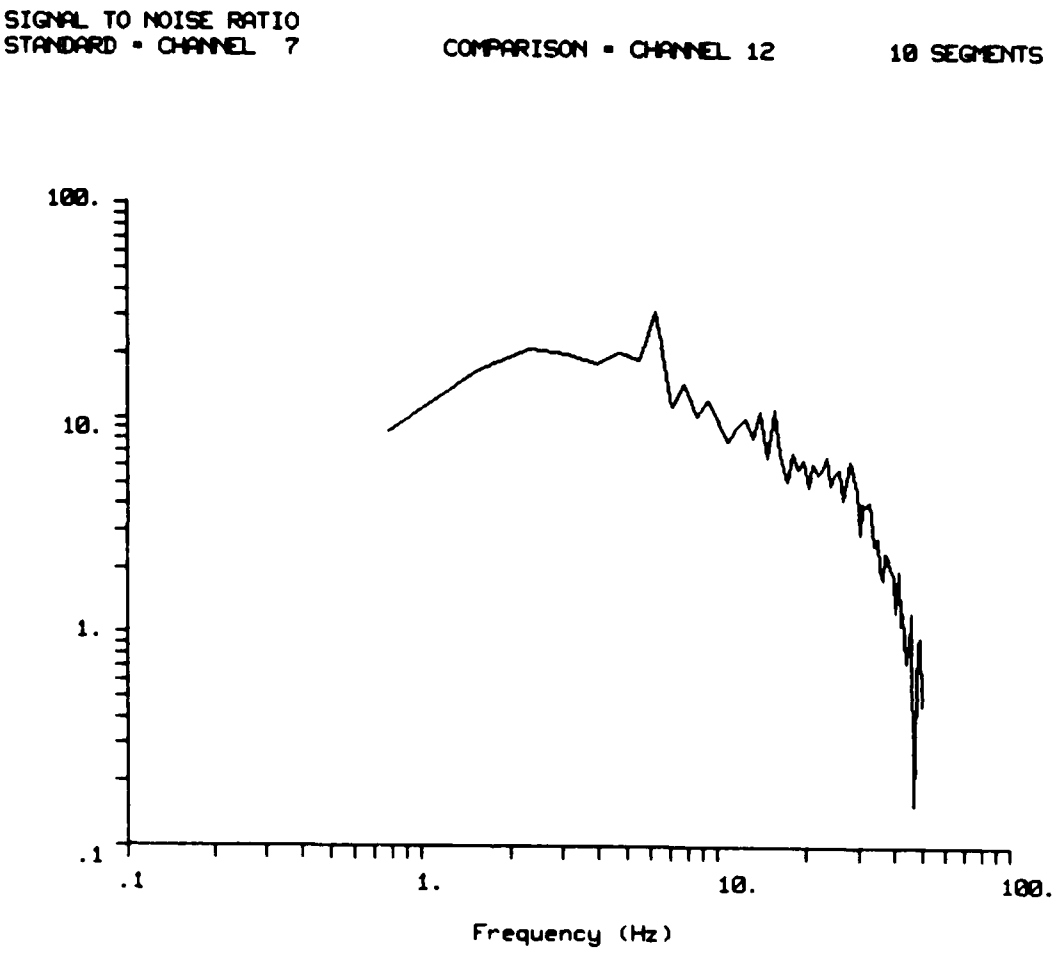

S/N ESTIMATE : LOW LEVEL MEASUREMENTS

Figure 5

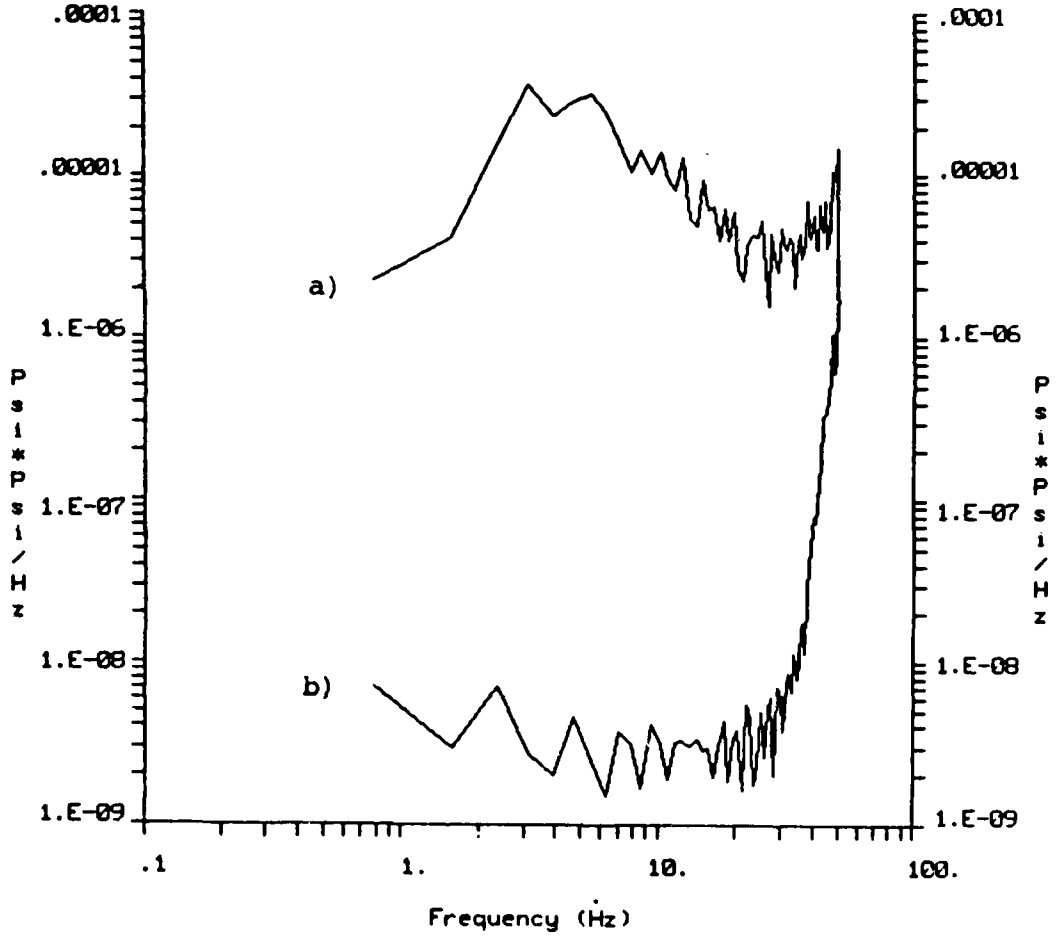

DOF=2

a) Total Spectra
b) Incoherent Portion

PRESSURE SPECTRA (HIGH LEVEL)

Figure 6

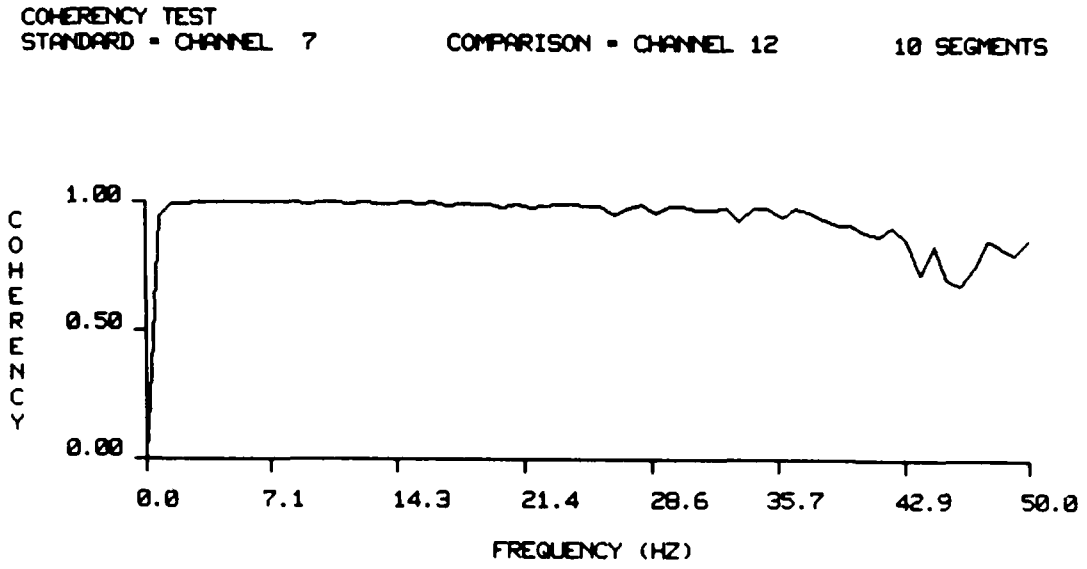

Sensor Separation ≈ 1 Meter

CHANNEL COHERENCY
HIGH LEVEL PRESSURE MEASUREMENTS

Figure 7

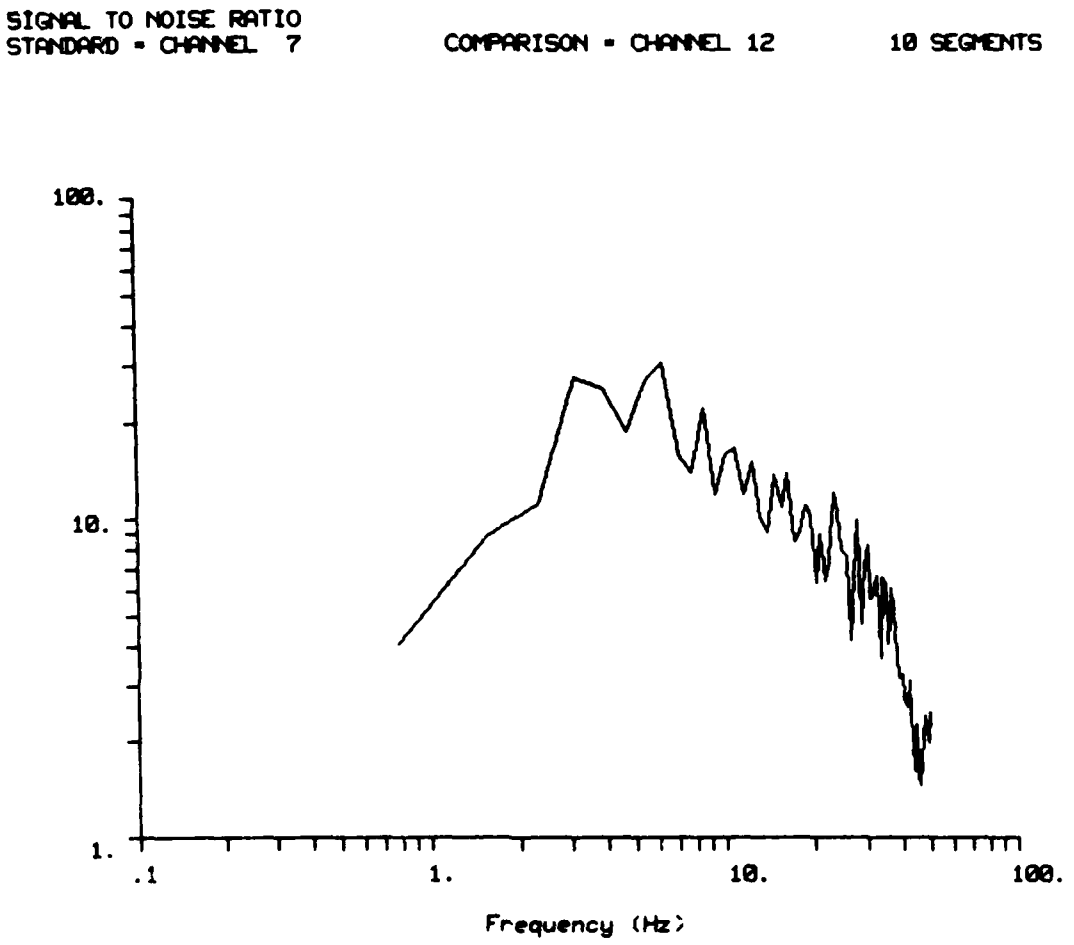

S/N ESTIMATE : HIGH LEVEL MEASUREMENTS

Figure 8

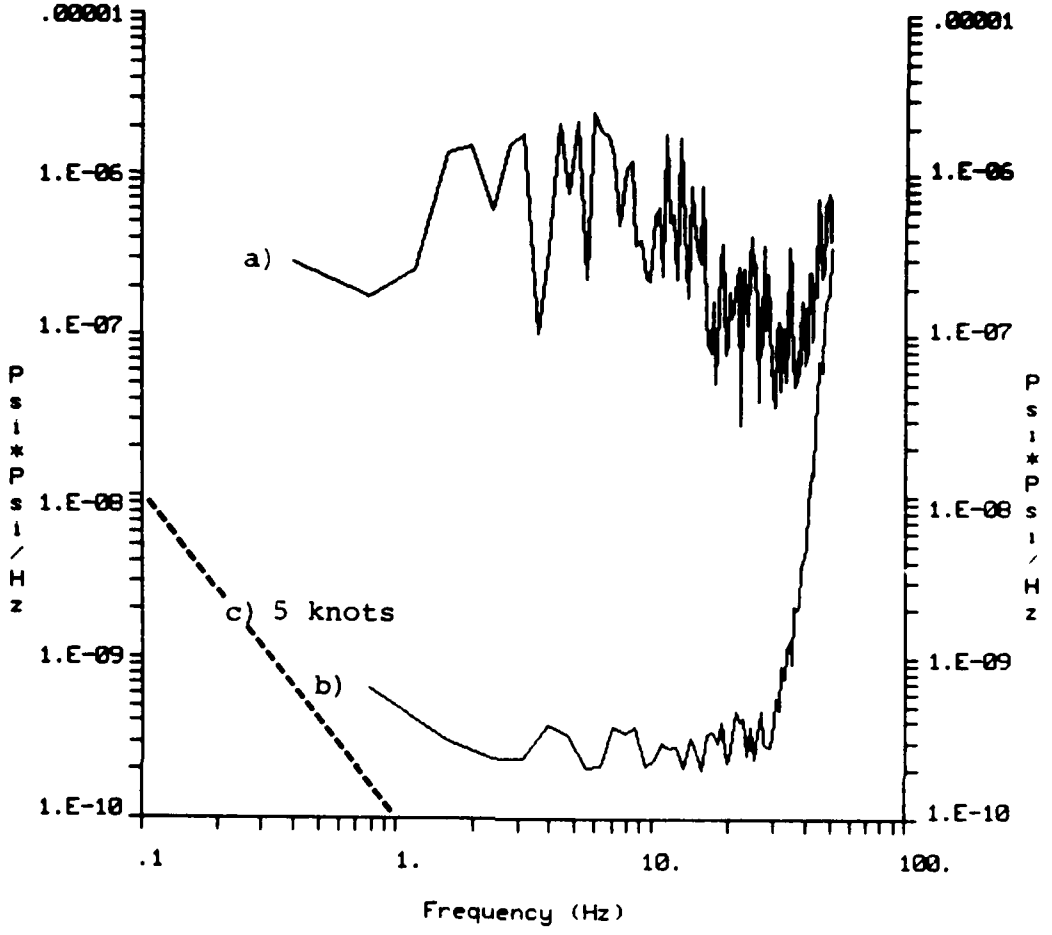

a) Spectral Average, Distance 293 Meters

b) System Noise Figure for Low Level Measurements

c) Pressure Spectrum for 5 Knot Wind

SPECTRA: MAIN ENGINE

Figure 9

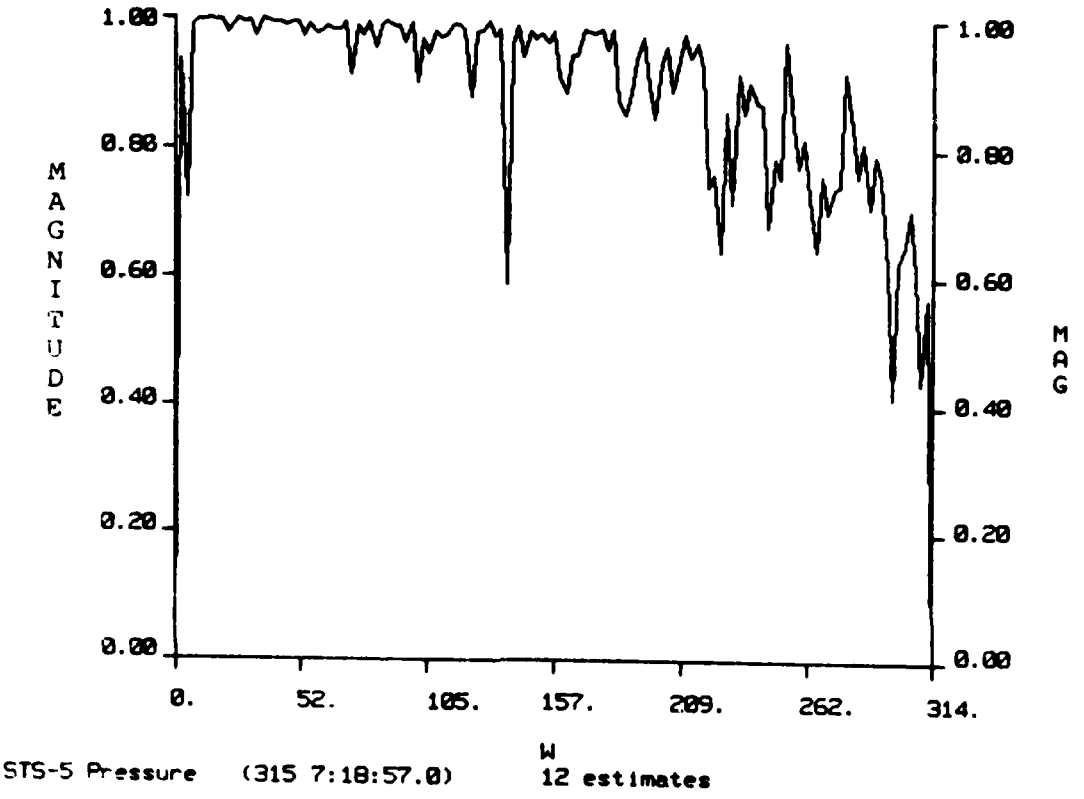

$\hat{v}(k,\omega)$: MAIN ENGINE

Figure 10

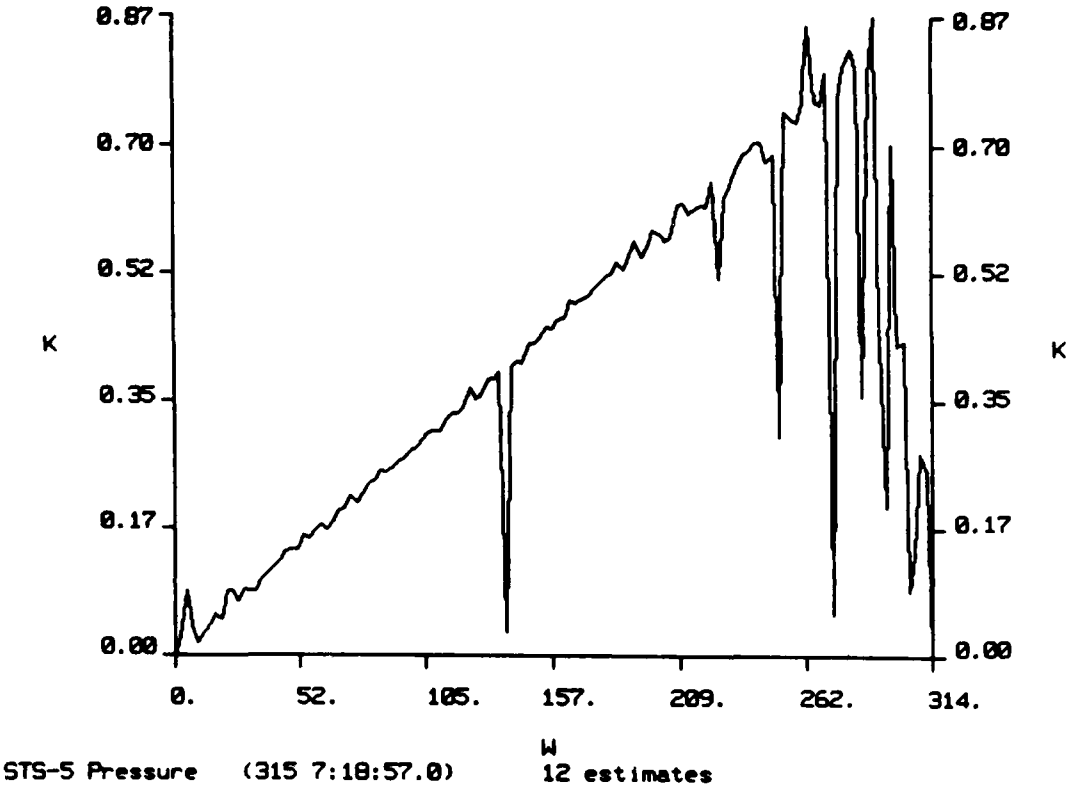

PROPAGATION CHARACTERISTIC: MAIN ENGINE

Figure 11

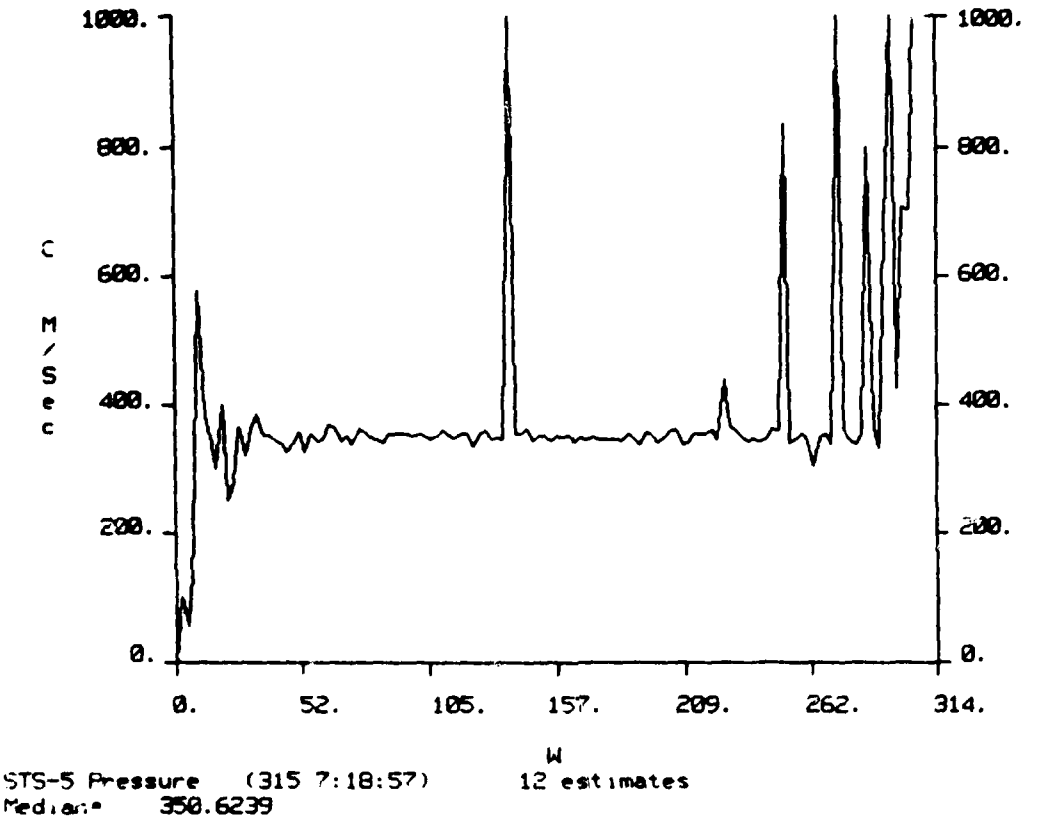

PHASE VELOCITY: MAIN ENGINE

Figure 12

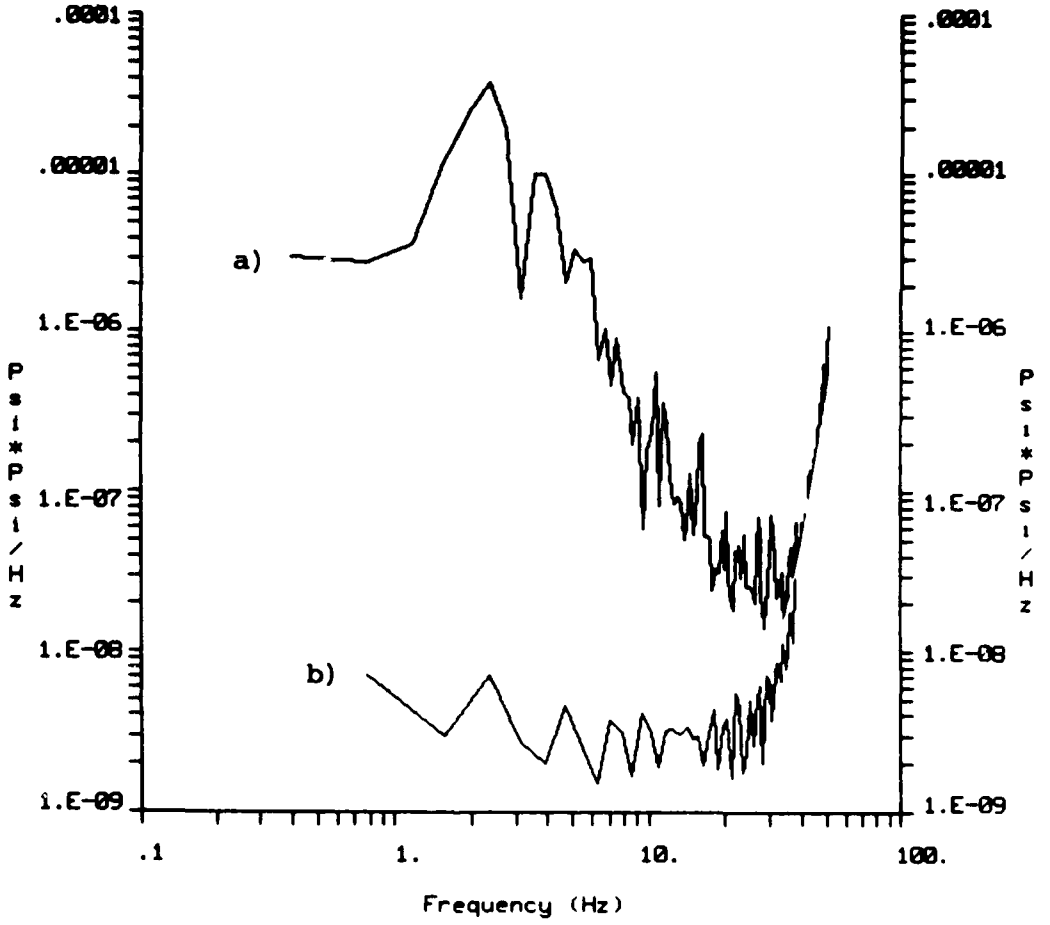

a) Spectral Average ~293 Meters DOF ~14

b) Noise Figure for High Level Measurements

SPECTRA: SOLIDS IGNITION

Figure 13

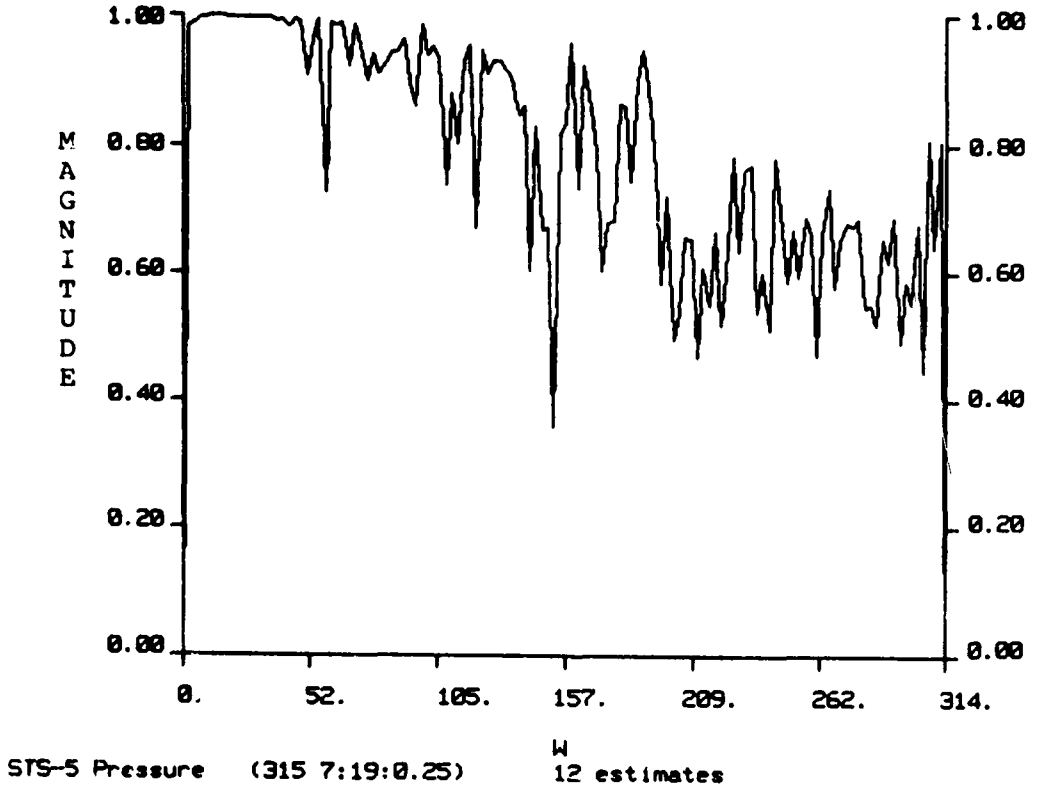

$\hat{v}(k,\omega)$: SOLIDS IGNITION

Figure 14

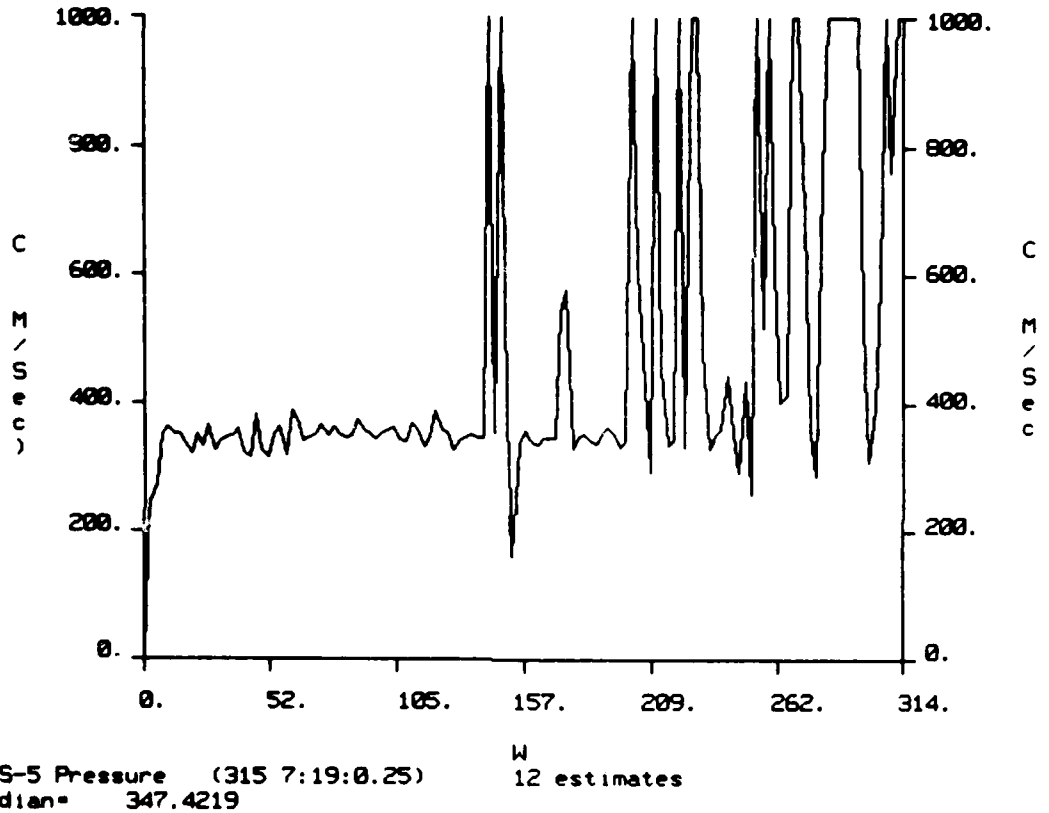

PHASE VELOCITY: SOLIDS IGNITION

Figure 15

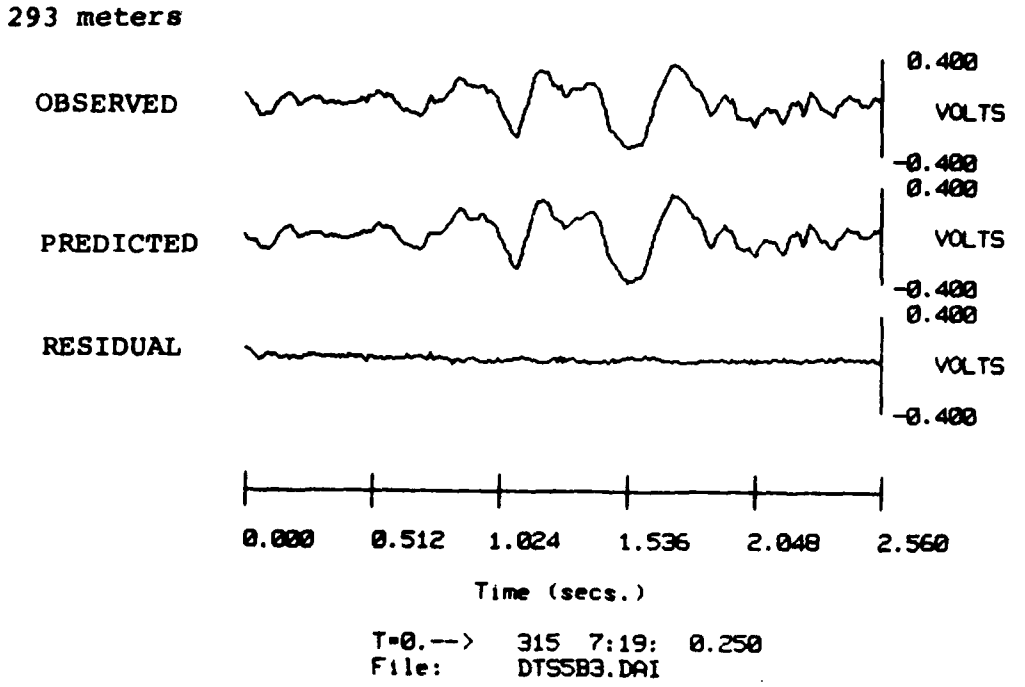

(Predicted pressure passed through Ch 6 response)

PRESSURE PREDICTION: SOLIDS IGNITION

Figure 16

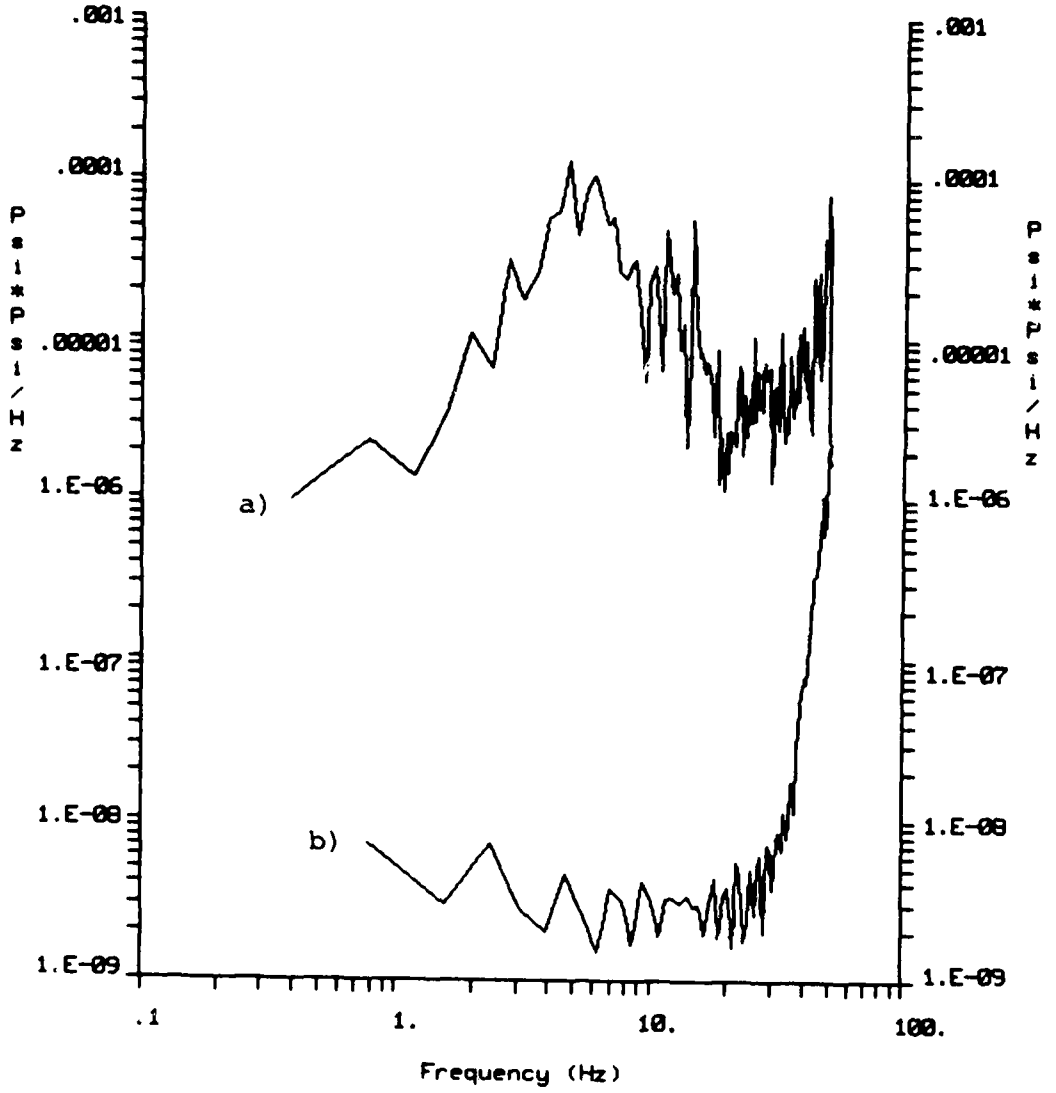

a) Spectral Average ~293 Meters DOF ~14
b) Noise Figure for High Level Measurements

SPECTRA: PLUME MAXIMUM

Figure 17

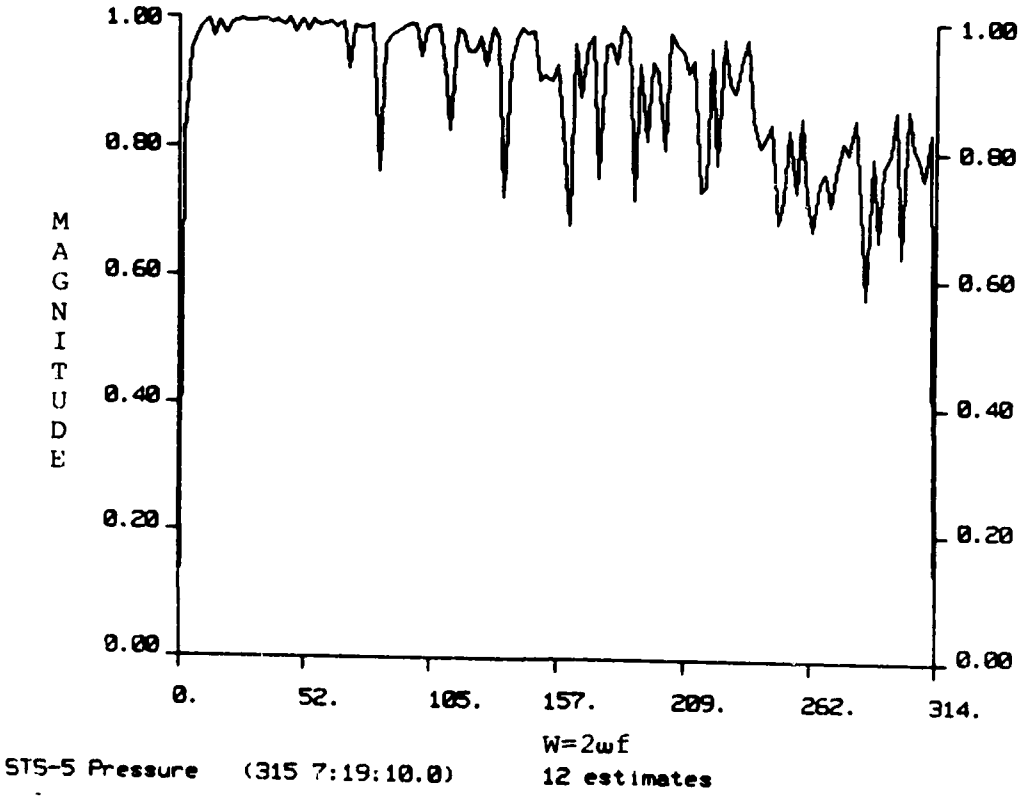

$\hat{v}(k,\omega)$: PLUME MAXIMUM

Figure 18

STS-5; KSC

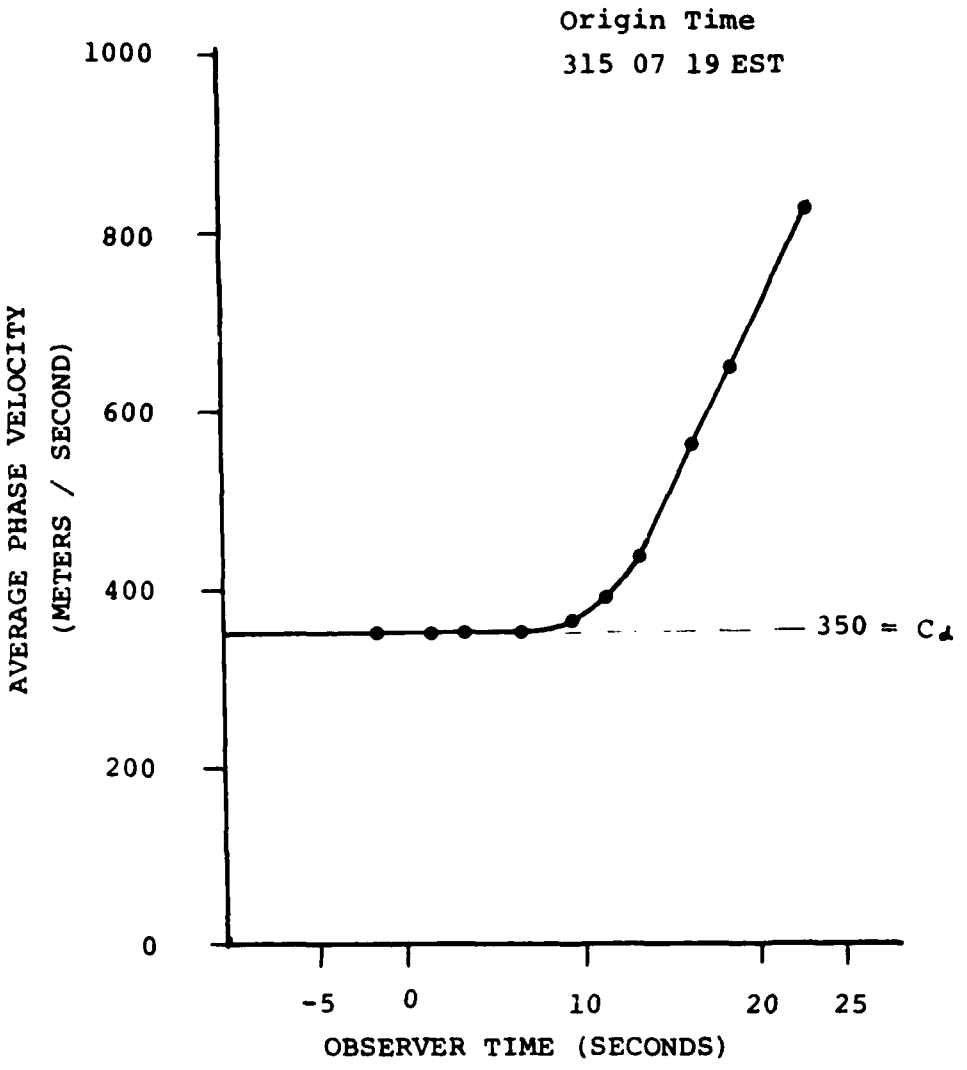

PHASE VELOCITY: STS-5 LAUNCH

Figure 19

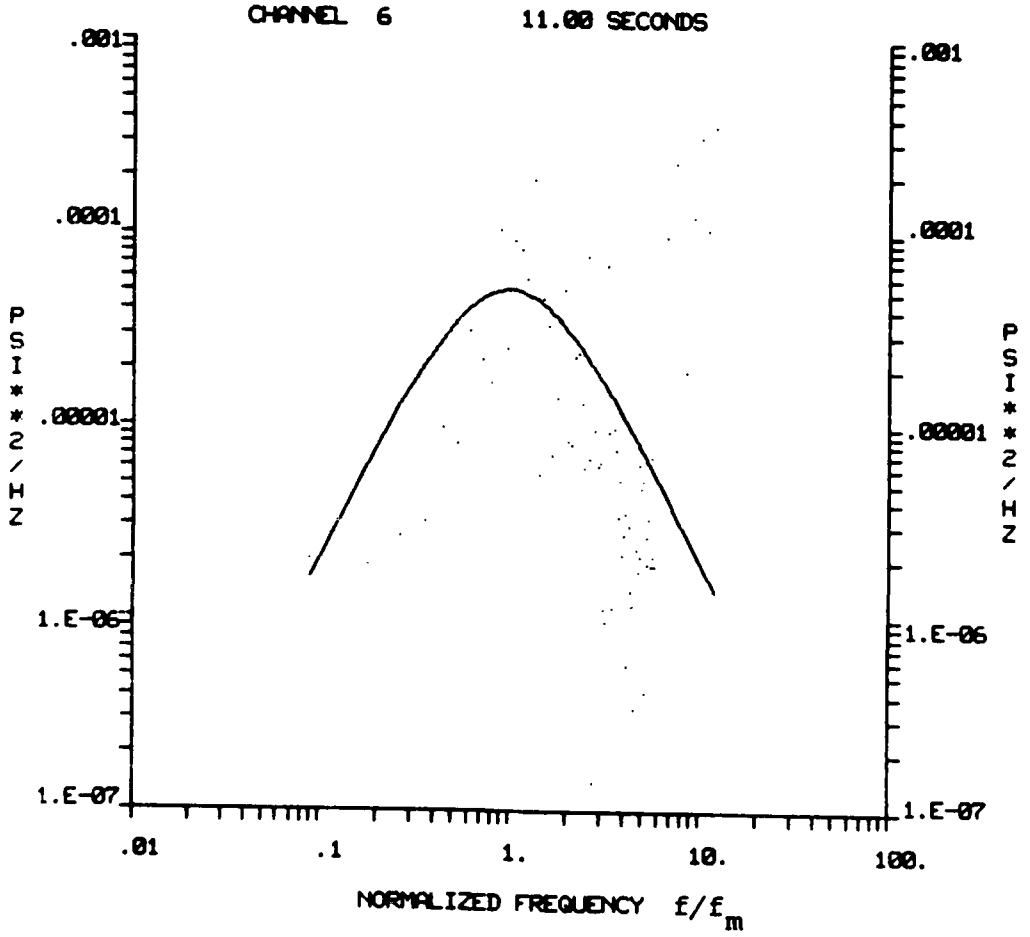

f_m = 4.368 Hz

STANDARD SPECTRUM: MAXIMUM OASPL

Figure 20

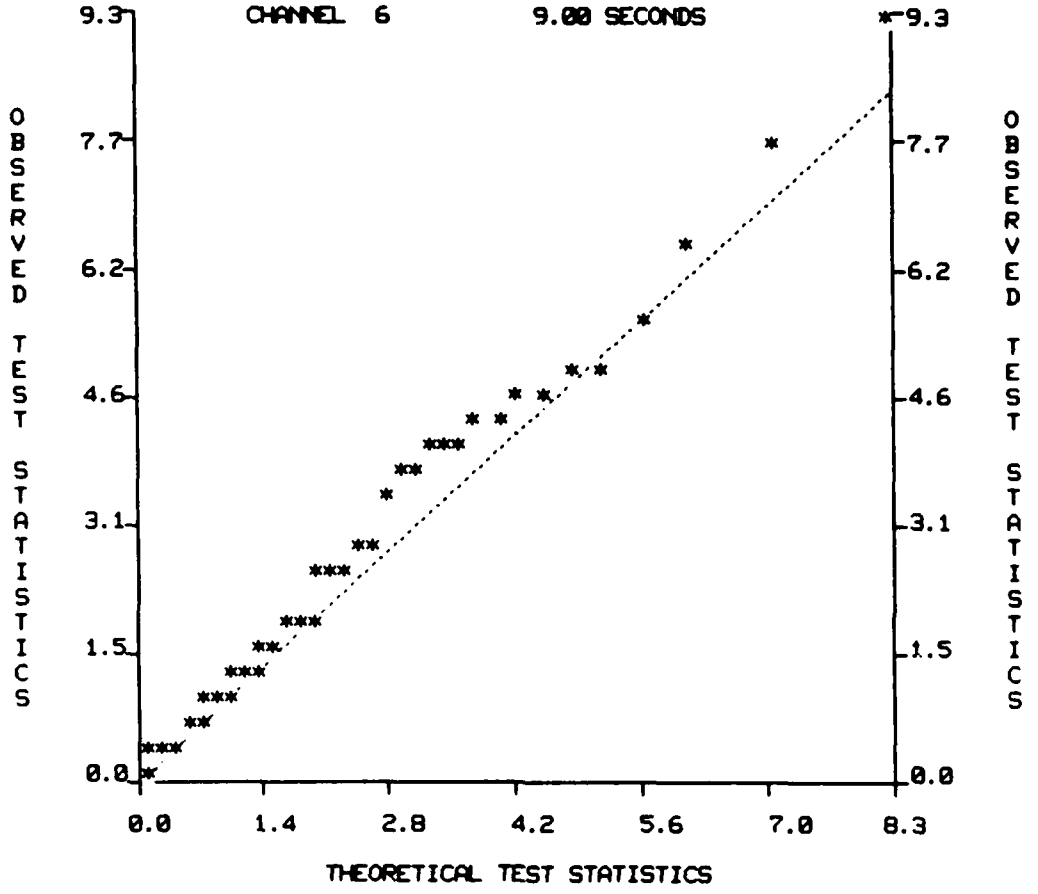

SPECTRUM ACCEPTANCE TEST

Figure 21

Maximum Power for a Ground Station at 300 Meters

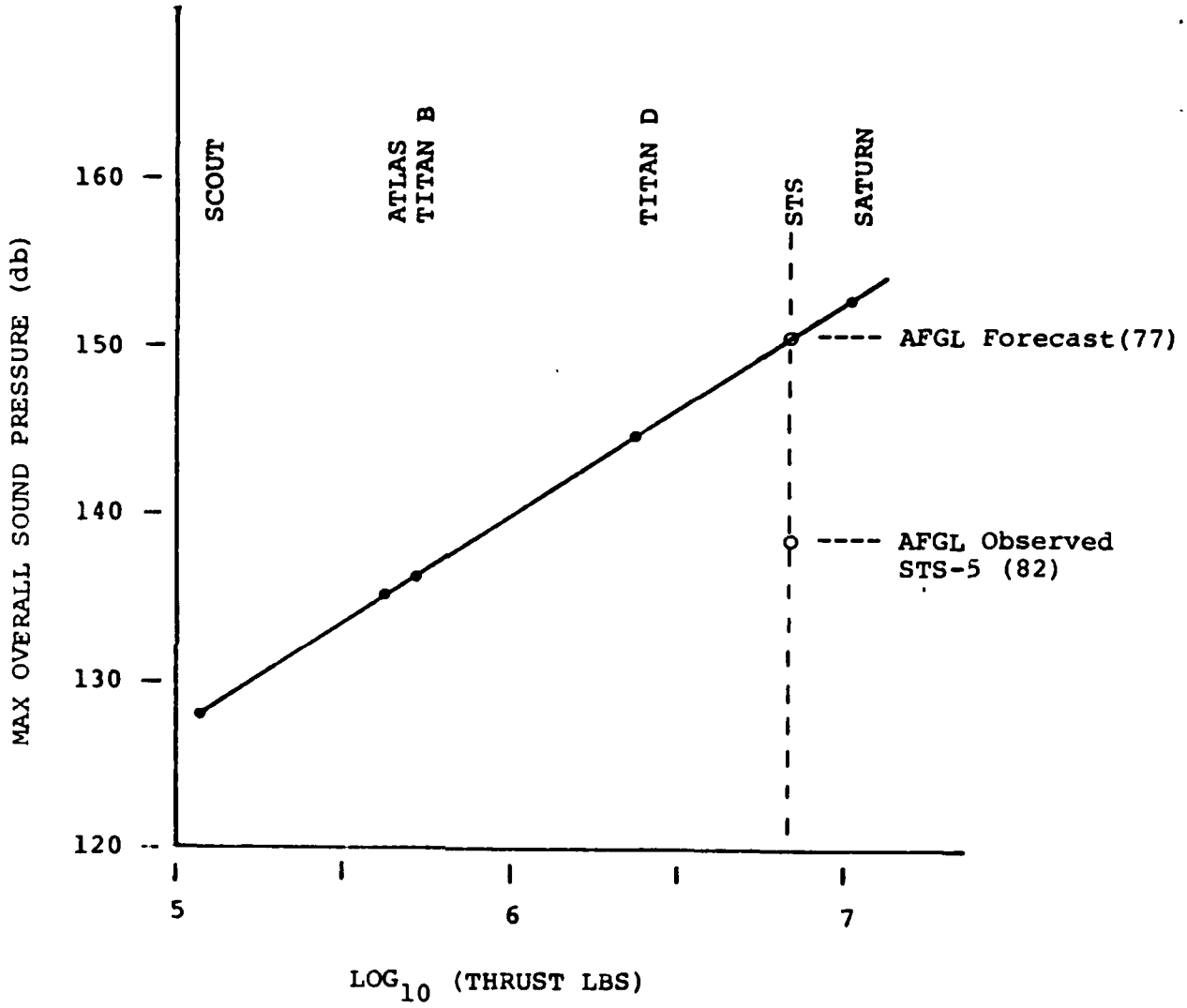

OASPL MAXIMA

Figure 22

10.0 APPENDIX A

COMMON MODE PRESSURE TEST # 8

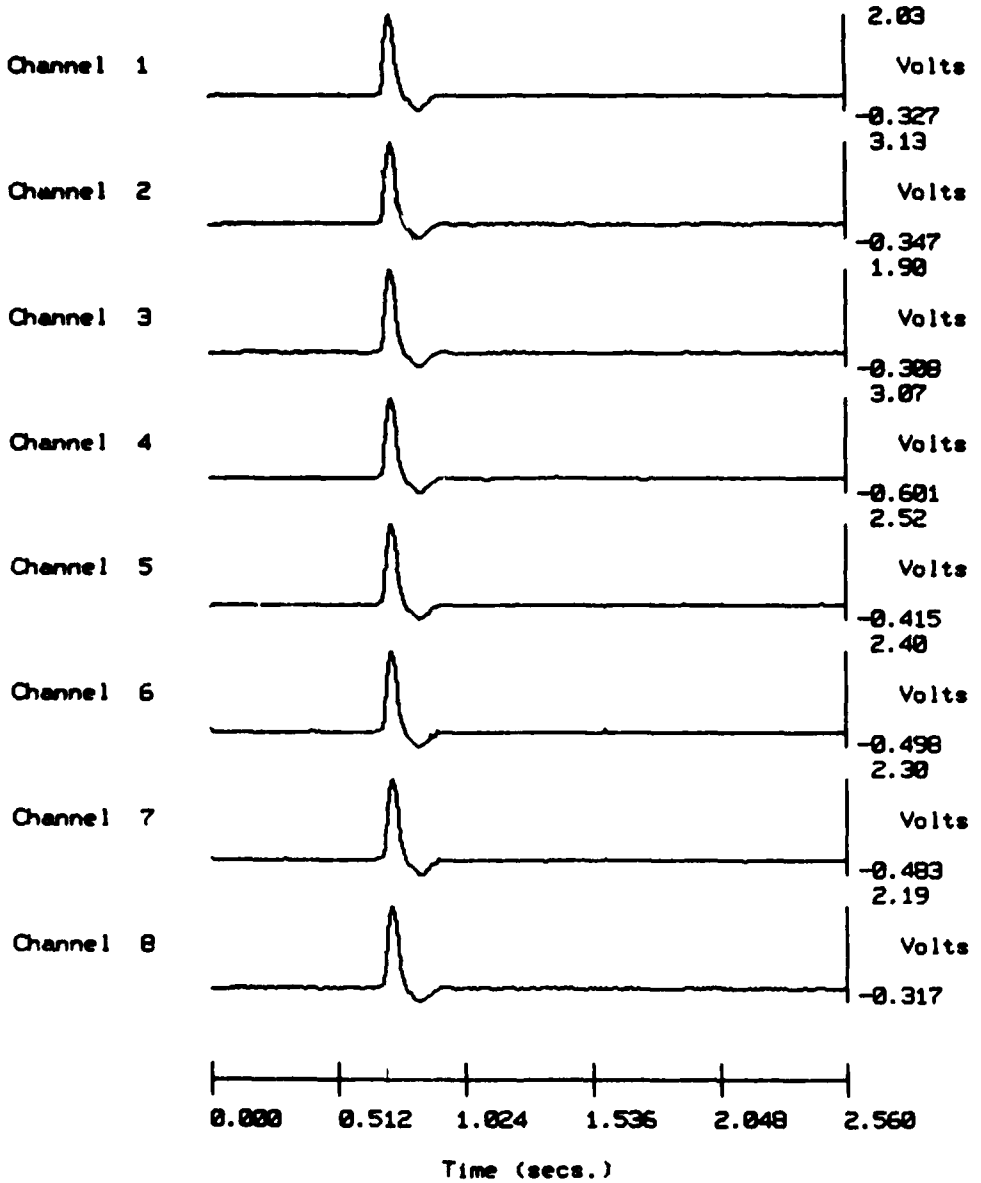
Channel 1
2.03
Volts
-0.327
Channel 2
3.13
Volts
-0.347
Channel 3
1.90
Volts
-0.308
Channel 4
3.07
Volts
-0.601
Channel 5
2.52
Volts
-0.415
Channel 6
2.40
Volts
-0.498
Channel 7
2.30
Volts
-0.483
Channel 8
2.19
Volts
-0.317
0.000
0.512
1.024
1.536
2.048
2.560
Time (secs.)
T=0.—> 315 12:39: 54.680
File: PRCAL8.DAI

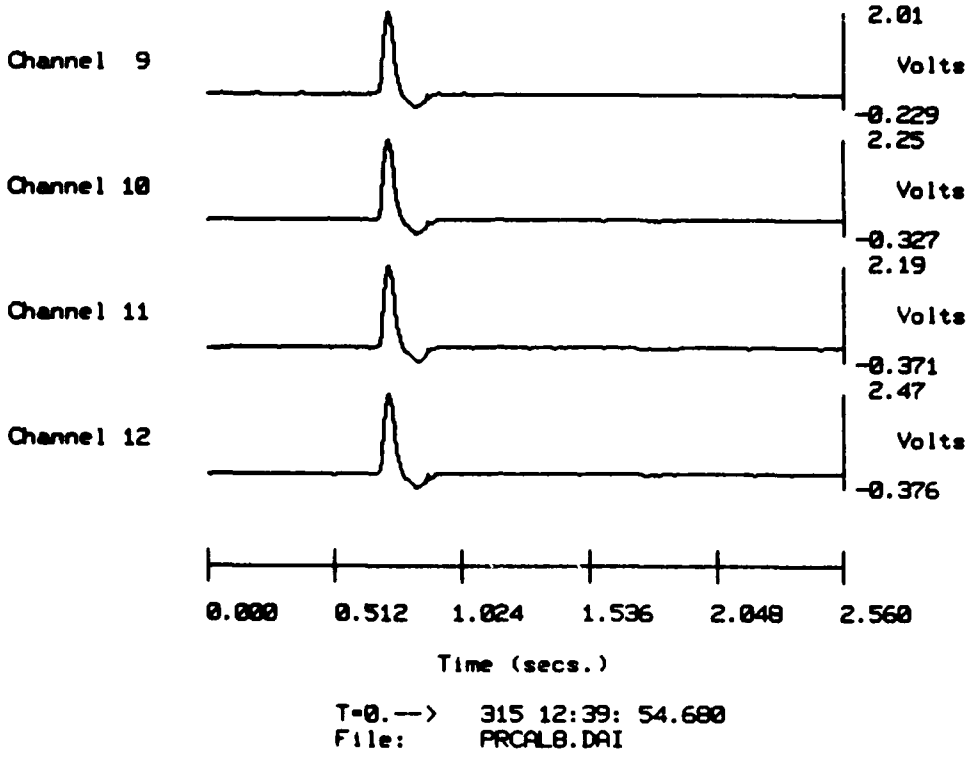
Channel 9
2.01
Volts
-0.229
Channel 10
2.25
Volts
-0.327
Channel 11
2.19
Volts
-0.371
Channel 12
2.47
Volts
-0.376
0.000
0.512
1.024
1.536
2.048
2.560
Time (secs.)
T=0.--> 315 12:39: 54.680
File: PRCAL8.DAI

10.0 APPENDIX A

HARDWARE RESPONSE FOR NOVEMBER 11, 1982
MEASUREMENTS AT KENNEDY SPACE CENTER (STS-5)

24-JAN-83
FILE: FLSTSS CHANNEL: 1 FILTER CARD: 1

SENSOR:

DC SCALE FACTOR	= 2.940	(VOLTS/PSI	)
DC PHASE (DEGREES)	= 180.0		
POLE FREQ (HZ)	= 2000.		

PREAMPLIFIER:

DC GAIN (DB)	= 5.894	DC PHASE (DEG)	= 0.0000
POLE FREQ (HZ)	= 100.0	DAMP COEFF	= 0.7070

FILTER:

STAGE 1

DC GAIN (DB)	= 7.969	DC PHASE (DEG)	= 0.0000
POLE FREQ (HZ)	= 670.0		

STAGE 2

DC GAIN (DB)	= 0.1217	DC PHASE (DEG)	= 180.0
POLE FREQ (HZ)	= 34.19	DAMP COEFF	= 1.009

STAGE 3

DC GAIN (DB)	= 0.3738E-02	DC PHASE (DEG)	= 0.0000
POLE FREQ (HZ)	= 34.34	DAMP COEFF	= 0.7320

STAGE 4

DC GAIN (DB)	= -0.8678E-02	DC PHASE (DEG)	= 180.0
POLE FREQ (HZ)	= 1591.		

STAGE 5

DC GAIN (DB)	= 0.6423E-01	DC PHASE (DEG)	= 180.0
POLE FREQ (HZ)	= 34.16	DAMP COEFF	= 0.2695

24-JAN-83
FILE: FLSTS5 CHANNEL: 2 FILTER CARD: 19

SENSOR:

DC SCALE FACTOR	= 4.402	(VOLTS/PSI	)
DC PHASE (DEGREES)	= 180.0		
POLE FREQ (HZ)	= 2000.		

PREAMPLIFIER:

DC GAIN (DB)	= 6.012	DC PHASE (DEG)	= 0.0000
POLE FREQ (HZ)	= 100.0	DAMP COEFF	= 0.7070

FILTER:

STAGE 1

DC GAIN (DB)	= 7.875	DC PHASE (DEG)	= 0.0000
POLE FREQ (HZ)	= 670.0		

STAGE 2

DC GAIN (DB)	= 0.3625E-01	DC PHASE (DEG)	= 180.0
POLE FREQ (HZ)	= 34.17	DAMP COEFF	= 1.003

STAGE 3

DC GAIN (DB)	= -0.2057E-01	DC PHASE (DEG)	= 0.0000
POLE FREQ (HZ)	= 34.34	DAMP COEFF	= 0.7288

STAGE 4

DC GAIN (DB)	= -0.5210E-02	DC PHASE (DEG)	= 180.0
POLE FREQ (HZ)	= 1592.		

STAGE 5

DC GAIN (DB)	= -0.2167E-01	DC PHASE (DEG)	= 180.0
POLE FREQ (HZ)	= 34.32	DAMP COEFF	= 0.2658

.....

24-JAN-83
FILE: FLSTS5 CHANNEL: 3 FILTER CARD: 3

SENSOR:

DC SCALE FACTOR =	2.762	(VOLTS/PSI	)
DC PHASE (DEGREES) =	180.0		
POLE FREQ (HZ) =	2000.		

PREAMPLIFIER:

DC GAIN (DB) =	6.129	DC PHASE (DEG) =	0.0000
POLE FREQ (HZ) =	100.0	DAMP COEFF =	0.7070

FILTER:

STAGE 1

DC GAIN (DB) =	7.952	DC PHASE (DEG) =	0.0000
POLE FREQ (HZ) =	670.0		

STAGE 2

DC GAIN (DB) =	0.1065E-01	DC PHASE (DEG) =	180.0
POLE FREQ (HZ) =	34.25	DAMP COEFF =	1.006

STAGE 3

DC GAIN (DB) =	0.3359E-01	DC PHASE (DEG) =	0.0000
POLE FREQ (HZ) =	34.25	DAMP COEFF =	0.7327

STAGE 4

DC GAIN (DB) =	-0.8687E-03	DC PHASE (DEG) =	180.0
POLE FREQ (HZ) =	1592.		

STAGE 5

DC GAIN (DB) =	0.1298E-01	DC PHASE (DEG) =	180.0
POLE FREQ (HZ) =	34.33	DAMP COEFF =	0.2689

24-JAN-83
FILE: FLSTS5 CHANNEL: 4 FILTER CARD: 4

SENSOR:

DC SCALE FACTOR	= 4.581	(VOLTS/PSI	)
DC PHASE (DEGREES)	= 180.0		
POLE FREQ (HZ)	= 2000.		

PREAMPLIFIER:

DC GAIN (DB)	= 6.034	DC PHASE (DEG)	= 0.0000
POLE FREQ (HZ)	= 100.0	DAMP COEFF	= 0.7070

FILTER:

STAGE 1

DC GAIN (DB)	= 7.945	DC PHASE (DEG)	= 0.0000
POLE FREQ (HZ)	= 670.0		

STAGE 2

DC GAIN (DB)	= 0.1546E-01	DC PHASE (DEG)	= 180.0
POLE FREQ (HZ)	= 34.35	DAMP COEFF	= 0.9983

STAGE 3

DC GAIN (DB)	= 0.1124E-01	DC PHASE (DEG)	= 0.0000
POLE FREQ (HZ)	= 34.33	DAMP COEFF	= 0.7325

STAGE 4

DC GAIN (DB)	= -0.7800E-02	DC PHASE (DEG)	= 180.0
POLE FREQ (HZ)	= 1589.		

STAGE 5

DC GAIN (DB)	= 0.5700E-01	DC PHASE (DEG)	= 180.0
POLE FREQ (HZ)	= 34.33	DAMP COEFF	= 0.2675

.....

24-JAN-83
FILE: FLSTS5 CHANNEL: 5 FILTER CARD: 5

SENSOR:

DC SCALE FACTOR =	3.813	(VOLTS/PSI	)
DC PHASE (DEGREES) =	180.0		
POLE FREQ (HZ) =	2000.		

PREAMPLIFIER:

DC GAIN (DB) =	5.990	DC PHASE (DEG) =	0.0000
POLE FREQ (HZ) =	100.0	DAMP COEFF =	0.7070

FILTER:

STAGE 1

DC GAIN (DB) =	7.912	DC PHASE (DEG) =	0.0000
POLE FREQ (HZ) =	670.0		

STAGE 2

DC GAIN (DB) =	-0.3960E-01	DC PHASE (DEG) =	180.0
POLE FREQ (HZ) =	34.29	DAMP COEFF =	1.002

STAGE 3

DC GAIN (DB) =	-0.4120E-01	DC PHASE (DEG) =	0.0000
POLE FREQ (HZ) =	34.46	DAMP COEFF =	0.7281

STAGE 4

DC GAIN (DB) =	-0.1216E-01	DC PHASE (DEG) =	180.0
POLE FREQ (HZ) =	1592.		

STAGE 5

DC GAIN (DB) =	0.5650E-01	DC PHASE (DEG) =	180.0
POLE FREQ (HZ) =	34.23	DAMP COEFF =	0.2688

24-JAN-83
FILE: FLSTS5 CHANNEL: 6 FILTER CARD: 6

SENSOR:

DC SCALE FACTOR	= 3.625	(VOLTS/PSI	)
DC PHASE (DEGREES)	= 180.0		
POLE FREQ (HZ)	= 2000.		

PREAMPLIFIER:

DC GAIN (DB)	= 6.042	DC PHASE (DEG)	= 0.0000
POLE FREQ (HZ)	= 100.0	DAMP COEFF	= 0.7070

FILTER:

STAGE 1

DC GAIN (DB)	= 7.984	DC PHASE (DEG)	= 0.0000
POLE FREQ (HZ)	= 670.0		

STAGE 2

DC GAIN (DB)	= -0.1287	DC PHASE (DEG)	= 180.0
POLE FREQ (HZ)	= 34.26	DAMP COEFF	= 1.004

STAGE 3

DC GAIN (DB)	= 0.9717E-01	DC PHASE (DEG)	= 0.0000
POLE FREQ (HZ)	= 34.19	DAMP COEFF	= 0.7345

STAGE 4

DC GAIN (DB)	= -0.1735E-01	DC PHASE (DEG)	= 180.0
POLE FREQ (HZ)	= 1591.		

STAGE 5

DC GAIN (DB)	= 0.1541E-01	DC PHASE (DEG)	= 180.0
POLE FREQ (HZ)	= 34.26	DAMP COEFF	= 0.2701

24-JAN-83
FILE: FLSTS5 CHANNEL: 7 FILTER CARD: 7

SENSOR:

DC SCALE FACTOR =	3.551	(VOLTS/PSI	)
DC PHASE (DEGREES) =	180.0		
POLE FREQ (HZ) =	2000.		

PREAMPLIFIER:

DC GAIN (DB) =	5.960	DC PHASE (DEG) =	0.0000
POLE FREQ (HZ) =	100.0	DAMP COEFF =	0.7070

FILTER:

STAGE 1

DC GAIN (DB) =	7.994	DC PHASE (DEG) =	0.0000
POLE FREQ (HZ) =	670.0		

STAGE 2

DC GAIN (DB) =	-0.2010E-01	DC PHASE (DEG) =	180.0
POLE FREQ (HZ) =	34.23	DAMP COEFF =	1.006

STAGE 3

DC GAIN (DB) =	0.1875E-02	DC PHASE (DEG) =	0.0000
POLE FREQ (HZ) =	34.28	DAMP COEFF =	0.7363

STAGE 4

DC GAIN (DB) =	-0.8681E-02	DC PHASE (DEG) =	180.0
POLE FREQ (HZ) =	1592.		

STAGE 5

DC GAIN (DB) =	0.5378E-01	DC PHASE (DEG) =	180.0
POLE FREQ (HZ) =	34.14	DAMP COEFF =	0.2681

24-JAN-83
FILE: FLSTS5 CHANNEL: 8 FILTER CARD: 8

SENSOR:

DC SCALE FACTOR	= 3.208	(VOLTS/PSI	)
DC PHASE (DEGREES)	= 180.0		
POLE FREQ (HZ)	= 2000.		

PREAMPLIFIER:

DC GAIN (DB)	= 6.094	DC PHASE (DEG)	= 0.0000
POLE FREQ (HZ)	= 100.0	DAMP COEFF	= 0.7070

FILTER:

STAGE 1

DC GAIN (DB)	= 7.949	DC PHASE (DEG)	= 0.0000
POLE FREQ (HZ)	= 670.0		

STAGE 2

DC GAIN (DB)	= -0.3142E-01	DC PHASE (DEG)	= 180.0
POLE FREQ (HZ)	= 34.39	DAMP COEFF	= 1.001

STAGE 3

DC GAIN (DB)	= -0.1691E-01	DC PHASE (DEG)	= 0.0000
POLE FREQ (HZ)	= 34.43	DAMP COEFF	= 0.7307

STAGE 4

DC GAIN (DB)	= -0.1129E-01	DC PHASE (DEG)	= 180.0
POLE FREQ (HZ)	= 1592.		

STAGE 5

DC GAIN (DB)	= 0.1737E-02	DC PHASE (DEG)	= 180.0
POLE FREQ (HZ)	= 34.43	DAMP COEFF	= 0.2661

.....

24-JAN-83
FILE: FLSTS5 CHANNEL: 9 FILTER CARD: 9

SENSOR:

DC SCALE FACTOR	= 2.917	(VOLTS/PSI	)
DC PHASE (DEGREES)	= 180.0		
POLE FREQ (HZ)	= 2000.		

PREAMPLIFIER:

DC GAIN (DB)	= 5.916	DC PHASE (DEG)	= 0.0000
POLE FREQ (HZ)	= 100.0	DAMP COEFF	= 0.7070

FILTER:

STAGE 1

DC GAIN (DB)	= 7.923	DC PHASE (DEG)	= 0.0000
POLE FREQ (HZ)	= 670.0		

STAGE 2

DC GAIN (DB)	= -0.3290E-01	DC PHASE (DEG)	= 180.0
POLE FREQ (HZ)	= 34.34	DAMP COEFF	= 1.002

STAGE 3

DC GAIN (DB)	= -0.7479E-02	DC PHASE (DEG)	= 0.0000
POLE FREQ (HZ)	= 34.31	DAMP COEFF	= 0.7333

STAGE 4

DC GAIN (DB)	= 0.2601E-02	DC PHASE (DEG)	= 180.0
POLE FREQ (HZ)	= 1588.		

STAGE 5

DC GAIN (DB)	= -0.1381E-01	DC PHASE (DEG)	= 180.0
POLE FREQ (HZ)	= 34.39	DAMP COEFF	= 0.2655

24-JAN-83
FILE: FLSTS5 CHANNEL: 10 FILTER CARD: 10

SENSOR:

DC SCALE FACTOR =	3.328	(VOLTS/PSI	)
DC PHASE (DEGREES) =	180.0		
POLE FREQ (HZ) =	2000.		

PREAMPLIFIER:

DC GAIN (DB) =	6.042	DC PHASE (DEG) =	0.0000
POLE FREQ (HZ) =	100.0	DAMP COEFF =	0.7070

FILTER:

STAGE 1

DC GAIN (DB) =	7.956	DC PHASE (DEG) =	0.0000
POLE FREQ (HZ) =	670.0		

STAGE 2

DC GAIN (DB) =	-0.4789E-01	DC PHASE (DEG) =	180.0
POLE FREQ (HZ) =	34.37	DAMP COEFF =	1.002

STAGE 3

DC GAIN (DB) =	0.3177E-01	DC PHASE (DEG) =	0.0000
POLE FREQ (HZ) =	34.26	DAMP COEFF =	0.7341

STAGE 4

DC GAIN (DB) =	0.1301E-01	DC PHASE (DEG) =	180.0
POLE FREQ (HZ) =	1589.		

STAGE 5

DC GAIN (DB) =	0.8568E-01	DC PHASE (DEG) =	180.0
POLE FREQ (HZ) =	34.16	DAMP COEFF =	0.2696

.....

24-JAN-83
FILE: FLSTSS CHANNEL: 11 FILTER CARD: 11

SENSOR:

DC SCALE FACTOR =	3.295	(VOLTS/PSI	)
DC PHASE (DEGREES) =	180.0		
POLE FREQ (HZ) =	2000.		

PREAMPLIFIER:

DC GAIN (DB) =	6.021	DC PHASE (DEG) =	0.0000
POLE FREQ (HZ) =	100.0	DAMP COEFF =	0.7070

FILTER:

STAGE 1

DC GAIN (DB) =	7.978	DC PHASE (DEG) =	0.0000
POLE FREQ (HZ) =	670.0		

STAGE 2

DC GAIN (DB) =	-0.6119E-01	DC PHASE (DEG) =	180.0
POLE FREQ (HZ) =	34.42	DAMP COEFF =	1.000

STAGE 3

DC GAIN (DB) =	-0.1127E-01	DC PHASE (DEG) =	0.0000
POLE FREQ (HZ) =	34.31	DAMP COEFF =	0.7340

STAGE 4

DC GAIN (DB) =	-0.1650E-01	DC PHASE (DEG) =	180.0
POLE FREQ (HZ) =	1593.		

STAGE 5

DC GAIN (DB) =	-0.7756E-01	DC PHASE (DEG) =	180.0
POLE FREQ (HZ) =	34.40	DAMP COEFF =	0.2678

24-JAN-83
FILE: FLSTSS CHANNEL: 12 FILTER CARD: 12

SENSOR:

DC SCALE FACTOR	= 3.595	(VOLTS/PSI	)
DC PHASE (DEGREES)	= 180.0		
POLE FREQ (HZ)	= 2000.		

PREAMPLIFIER:

DC GAIN (DB)	= 6.042	DC PHASE (DEG)	= 0.0000
POLE FREQ (HZ)	= 100.0	DAMP COEFF	= 0.7070

FILTER:

STAGE 1

DC GAIN (DB)	= 7.980	DC PHASE (DEG)	= 0.0000
POLE FREQ (HZ)	= 670.0		

STAGE 2

DC GAIN (DB)	= 0.1116E-02	DC PHASE (DEG)	= 180.0
POLE FREQ (HZ)	= 34.38	DAMP COEFF	= 1.002

STAGE 3

DC GAIN (DB)	= 0.9406E-02	DC PHASE (DEG)	= 0.0000
POLE FREQ (HZ)	= 34.40	DAMP COEFF	= 0.7322

STAGE 4

DC GAIN (DB)	= 0.8682E-02	DC PHASE (DEG)	= 180.0
POLE FREQ (HZ)	= 1590.		

STAGE 5

DC GAIN (DB)	= -0.2719E-01	DC PHASE (DEG)	= 180.0
POLE FREQ (HZ)	= 34.37	DAMP COEFF	= 0.2679

10.1 APPENDIX B: GLOSSARY OF TERMS

A	Angstroms
AFGL	Air Force Geophysics Laboratory
C	Phase Velocity
C_a	Speed of Sound in Air
db	Decibel: ref to .0002 dynes per sq. cm.
DOF	Degrees of freedom
f_m	Frequency of $G_{pp}(f)$ maximum
f_N	Nyquist frequency
GDAS	Geokinetic Data Acquisition System
$G_{pp}(f)$	Theoretical undeflected plume spectrum
i	$\sqrt{-1}$
k	Wave number
KSC	Kennedy Space Center
NASA	National Aeronautics & Space Administration
OASPL	Overall sound power level
p(p-p)	Peak to peak pressure
$p(r_\ell,t)$	Pressure at distance r_ℓ at time t
$p(r_\ell, \omega)$	Fourier transform of $p(r_\ell,t)$
PSI	Pressure, pounds per sq. in.
ScF	Scale factor
SD	Space Division
S/N	Signal to noise ratio
STS	Space Transportation System

VAFB	Vandenberg Air Force Base
Vo (p-p)	Peak to peak volts
$\ell(k, \omega)$	Ratio of magnitude of k weighted sum to scalar sum for $p(r_\ell, \omega)$
$\hat{\ell}(k, \omega)$	Absolute maximum of $\ell(k, \omega)$
ϕ_s	Source phase
τ_p	Phase time delay
ω	2π of angular frequency ($2\pi f$)

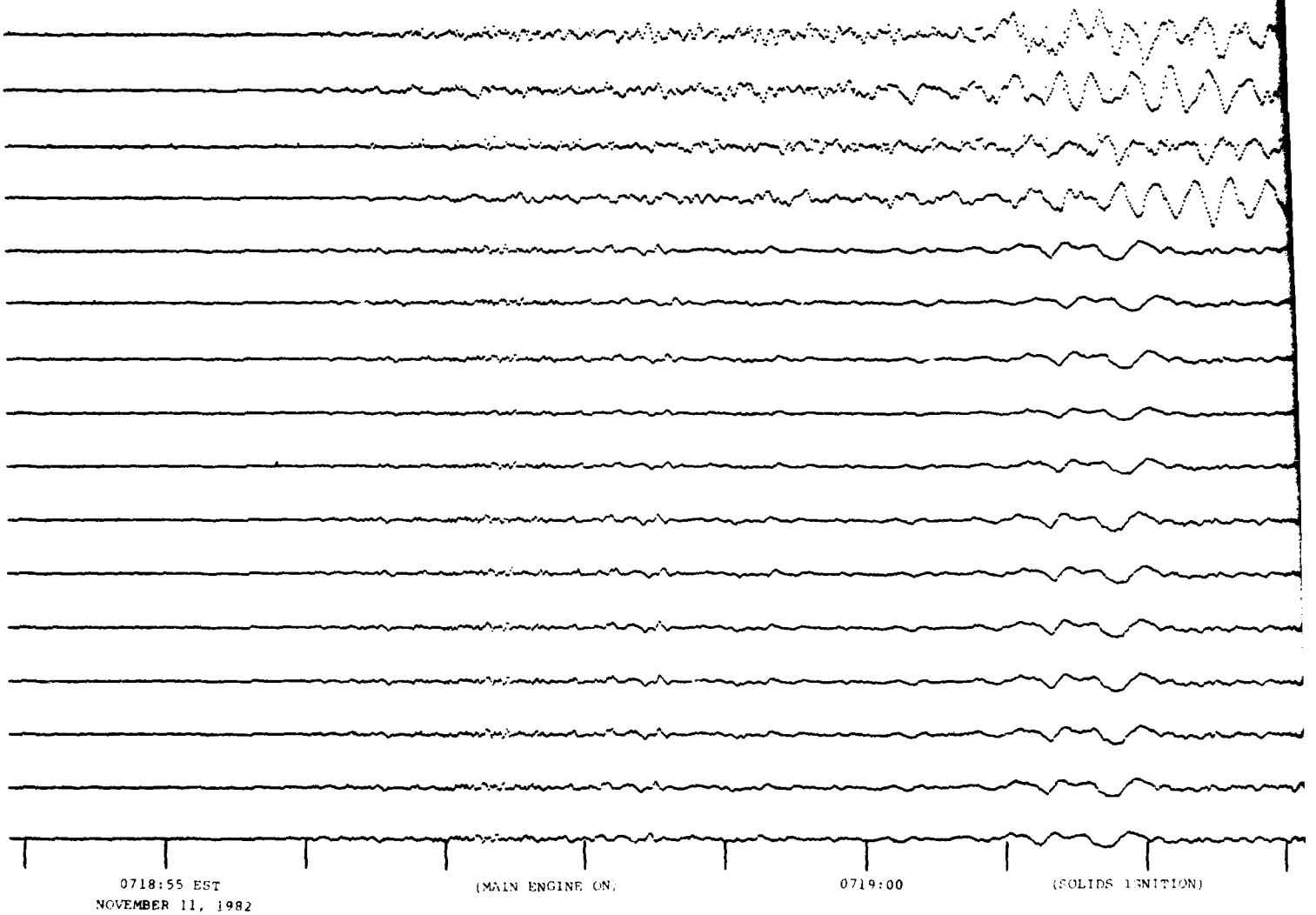
0718:55 EST
NOVEMBER 11, 1982
(MAIN ENGINE ON)
0719:00
(SOLIDS IGNITION)

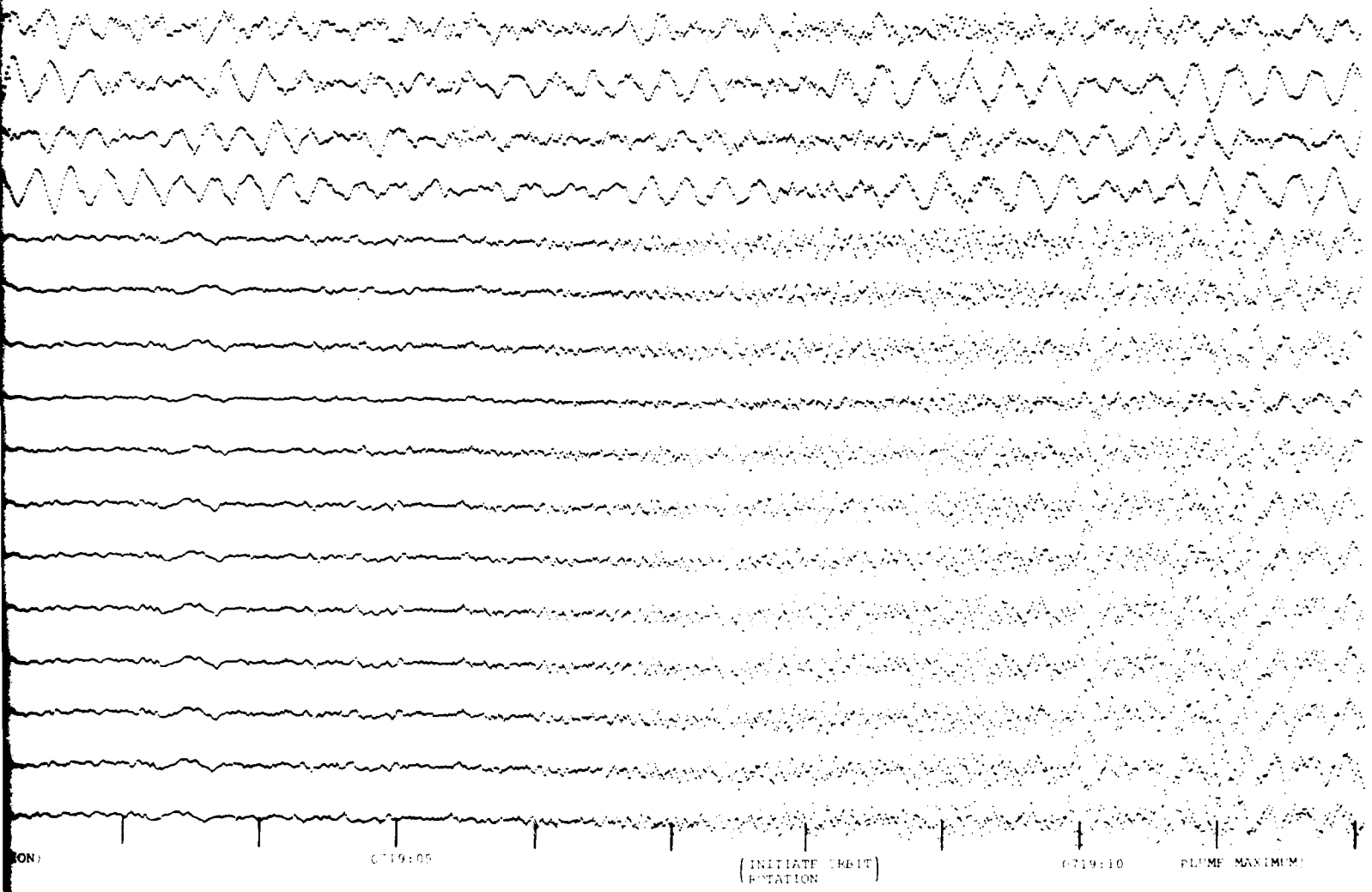

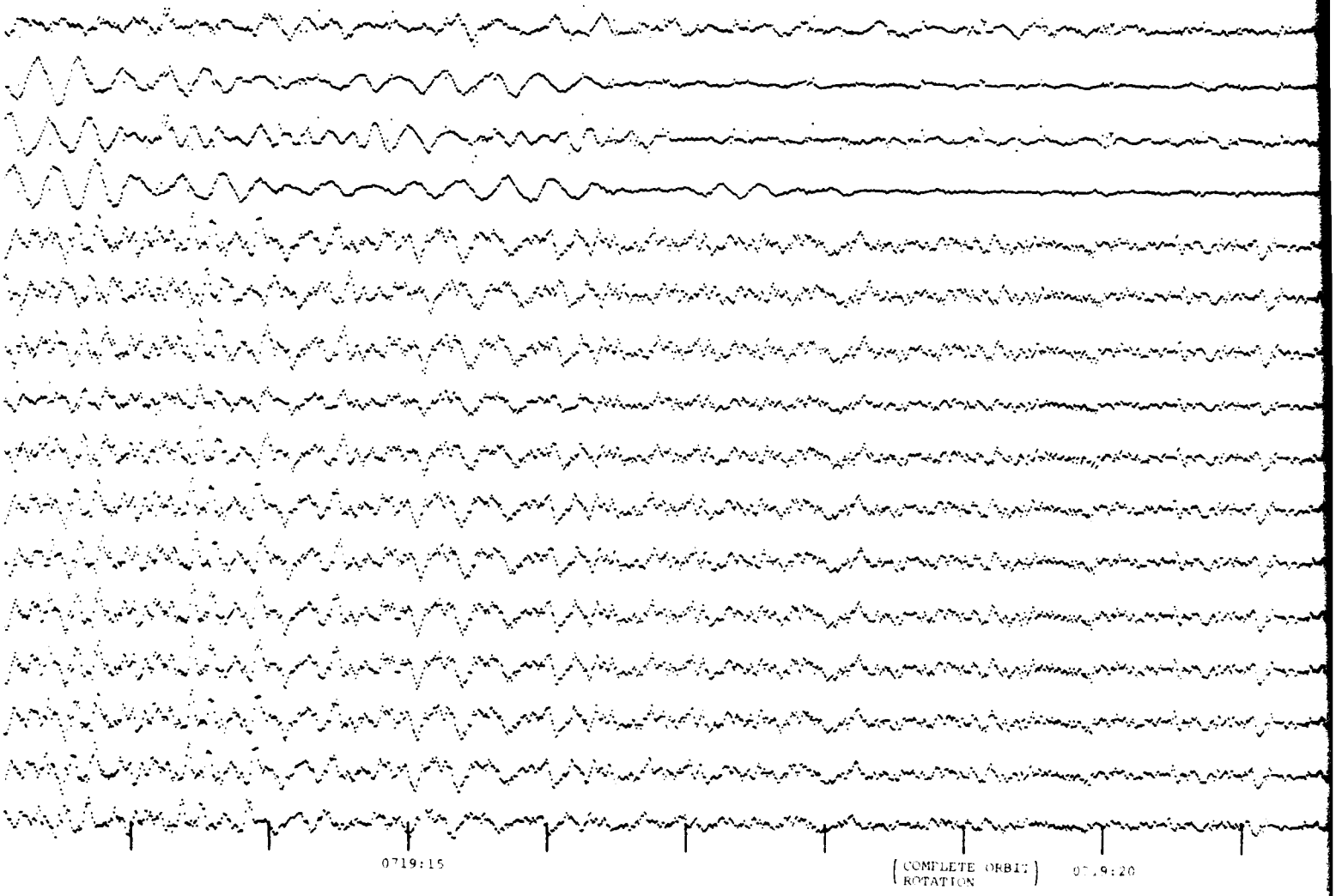
0719:15
COMPLETE ORBIT ROTATION
0719:20

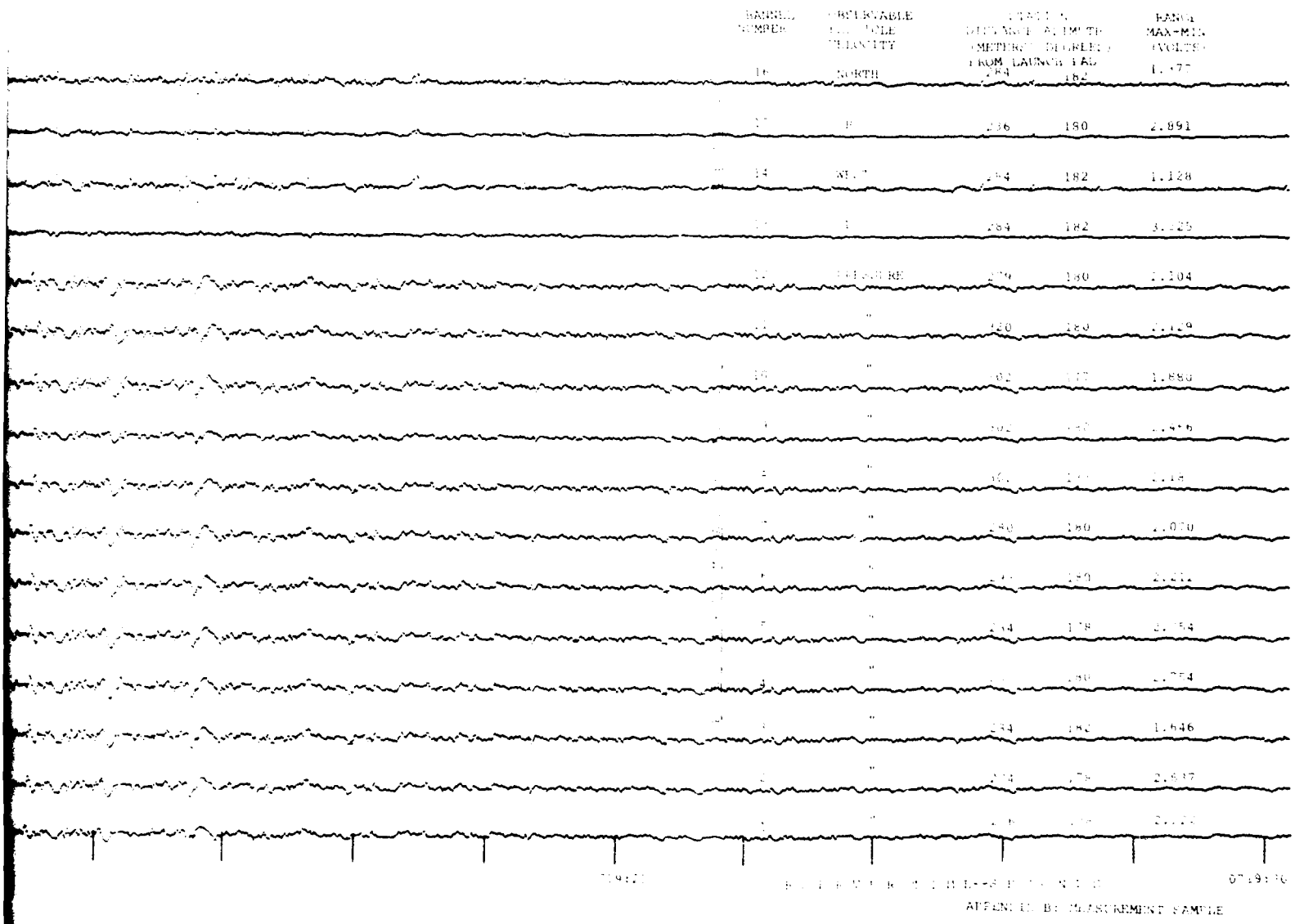
BARREL NUMBER
OBSERVABLE AT THE VOLE PLANVITY
RANGE (METERS) FROM LAUNCH PAD
AZIMUTH (DEGREES)
RANGE MAX-MIN (VOLTS)
NORTH
284 182 1.47
286 180 2.891
284 182 1.128
284 182 3.125
280 180 2.304
280 180 2.129
280 180 1.880
280 180 2.070
284 178 2.154
284 182 1.646
284 178 2.017
07:09:10
APPENDIX B: MEASUREMENT SAMPLE